Exploring aggregation-inducers for tau protein

Carlota de Galrinho e Silva

Thesis to obtain the Master of Science Degree in

Pharmaceutical Engineering

Supervisors:

Dr. Ana Margarida Pereira de Melo

Dr. Ana Margarida Nunes da Mata Pires de Azevedo

Examination Committee

Chairperson: Dr. Carla da Conceição Caramujo Rocha de Carvalho

Supervisor: Dr. Ana Margarida Pereira de Melo

Members of the Committee: Dr. Fábio Monteiro Fernandes

October 2023

Declaration

I declare that this document is an original work of my own authorship and that it fulfills all the requirements of the Code of Conduct and Good Practices of the Universidade de Lisboa.

Preface

The experimental work was developed at the Institute of Bioengineering and Biosciences of the Instituto Superior Técnico of the Universidade de Lisboa during the period February-October 2023, under the supervision of Dra. Ana Margarida Pereira de Melo and Dra. Ana Margarida Nunes daMata Pires de Azevedo. The experimental work was performed in the framework of the project 2022.01454.PTDC (funded by Foundation for Science and Technology (FCT)) and also Maria de Sousa Prize- 2nd Edition to Ana Melo (sponsored by Bial Foundation and Portuguese Medical Association).

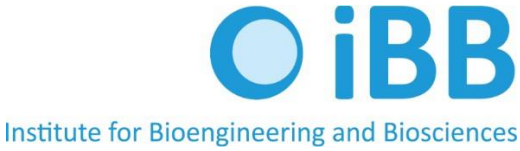

Acknowledgements

I would like to thank my supervisor, Professor Ana Melo, for the guidance and help she gave me during the project and also like to thank Professor Ana Azevedo. Also, I am grateful for the availability given to me.

I would also like to thank Rita Santos and to Jorge João in the lab at South Tower for helping me when I reached out for their help.

Next, I want to thank my family for all the effort they put into my education and all the support given.

To all my friends and to all the amazing people I met during my journey in the lab, thank you for keeping me company and for helping me.

Abstract

Tau is a neuronal intrinsically disordered and also microtubule-associated protein, whose abnormal deposition in the brain is linked to numerous neurogenerative diseases. These Tauopathies include Alzheimer's disease and frontotemporal dementia (with over 20 disorders). Several disease mutations in Tau, including P301L, impair Tau function (the binding and stabilization of microtubules) and also promote its pathological aggregation (both loss- and gain-of-function). The fibrillation of Tau *in vitro* has been extensively explored by Thioflavin T (ThT) fluorescence studies performed with the aggregation-prone K18 Tau fragment, comprising only the microtubule-binding domain. Moreover, the aggregation of the longest Tau isoform - 2N4R- in the presence of aggregation-inducers has been largely overlooked. Here, we investigated the effects of two anionic aggregation promoters - heparin and anionic lipid vesicles - in the fibrillation of wild-type (WT) and P301L 2N4R Tau proteins. Initially, both WT and P301L variants were recombinantly expressed and purified. Then, ThT fluorescence assays were carried out for both proteins in solution and in the presence of heparin or phosphatidylserine-containing membranes. Our assays show some variability in the absolute ThT signal, but globally our data indicate that heparin works as a stronger aggregation-promoter for both WT and P301L Tau than anionic lipid vesicles (here minor effects). Moreover, heparin has a higher aggregation effect in the P301L Tau protein.

Keywords: Alzheimer's disease, Tau Protein, Heparin, Lipid membranes and Thioflavin-T

Resumo

Tau é uma proteína neuronal intrinsecamente desordenada e também associada a microtúbulos, cuja deposição anormal no cérebro está ligada a inúmeras doenças neurodegenerativas. Estas Tauopatias incluem a doença de Alzheimer e a demência frontotemporal (com mais de 20 doenças). Várias mutações de doenças na Tau, incluindo P301L, prejudicam a função da Tau (ligação e estabilização dos microtúbulos) e também promovem a sua agregação patológica (perda ou ganho de função). A fibrilação da Tau *in vitro* foi extensivamente explorada por estudos de fluorescência com Tioflavina-T (ThT) realizados com o fragmento propenso à agregação K18 de Tau, compreendendo apenas o domínio de ligação aos microtúbulos. Além disso, a agregação da isoforma mais longa de Tau - 2N4R - na presença de indutores de agregação tem sido largamente ignorada. Aqui, investigamos os efeitos de dois promotores de agregação aniónicos - heparina e vesículas lipídicas aniónicas - na fibrilação de proteínas Tau do tipo wild-type (WT) e com a mutação P301L. Inicialmente, ambas as variantes WT e P301L foram expressas e purificadas de forma recombinante. Em seguida, foram realizados ensaios de fluorescência com ThT para ambas as proteínas em solução e na presença de heparina ou membranas contendo fosfatidilserina. Os nossos ensaios apresentam alguma variabilidade no sinal absoluto da ThT, mas globalmente os dados indicam que a heparina funciona como um promotor de agregação mais forte para WT e P301L Tau do que vesículas lipídicas aniónicas (aqui com efeitos menores). Além disso, a heparina tem um efeito maior na agregação da proteína P301L Tau.

Palavras-chave: Doença de Alzheimer, Proteína Tau, Heparina, Membranas Lipídicas e Tioflavina-T

Table of contents

List of figures

List of Tables

Abbreviations

3R Tau – Tau isoforms with three microtubule-binding repeat

4R Tau - Tau isoforms with four microtubule-binding repeats

Aβ - Amyloid β protein

AD - Alzheimer's disease

FTD - Frontotemporal dementia

FTDP-17 - Frontotemporal Dementia and Parkinsonism Linked to Chromosome 17

SDS-PAGE - Sodium Dodecyl Sulfate-polyacrylamide Gel Electrophoresis

Tau - Tubulin-associated Unit

MTBDs - Microtubule-binding Repeat Domains

NFTs - Neurofibrillary Tangles

WT - Wild Type

AFM - Atomic Force Microscopy

Amp - Ampicillin

CD - Circular Dichroism

DTT - Dithiothreitol

EDTA - Ethylenediamine N'-tetraacetic acid

His-Tag - Poly-Histidine Peptides

IMAC - Immobilized Metal Affinity Chromatography

IPTG - Isopropyl β-D-1-thiogalactopyranoside

MW - Molecular Weight

NMR - Nuclear Magnetic Resonance

OD - Optical Density

PMSF - Phenylmethanesulfonyl Fluoride

SDS-PAGE - Sodium Dodecyl Sulfate-Polyacrylamide Gel Electrophoresis

SEC - Size Exclusion Chromatography

TEV - Tobacco Etch Virus

Abs280nm - Absorbance at 280nm

Cryo-EM - Cryo-electron Microscopy

ThT - Thioflavin T

TEM - Transmission Electron Microscopy

FTIR - Fourier Transform Infrared Spectroscopy

LUVs – Large Unilamellar Vesicles

O/N - Overnight

POPC - 1-palmitoyl-2-oleoyl-*sn*-glycero-3-phosphocholine

POPS - 1-palmitoyl-2-oleoyl-sn-glycero-3-phospho-L-serine

1. Introduction

1.1. Alzheimer's disease (AD)

Neurodegenerative diseases are a set of severe disorders of the central nervous system, characterized by a progressive neuronal loss [1]. Alzheimer's disease (AD) represents the most common neurodegenerative disease in the elderly population and is becoming one of the most lethal diseases of this century [2]. This disorder is characterized by the presence of abundant extracellular amyloid plaques of β-amyloid peptide (Aβ) and aggregation of Tau protein into neurofibrillary tangles in neurons [3, 4]. Aβ results from the proteolytic cleavage of the amyloid precursor protein (APP) by a complex family of enzymes (γ¬secretases and β¬secretases), including presenilin 1 (PS1) and PS2 [4].

AD affects large areas of the cerebral cortex and hippocampus, and abnormalities are usually detected first in brain tissue surrounding the frontal and temporal lobes and subsequently progress to other areas of the neocortex at rates that vary between individuals [4].

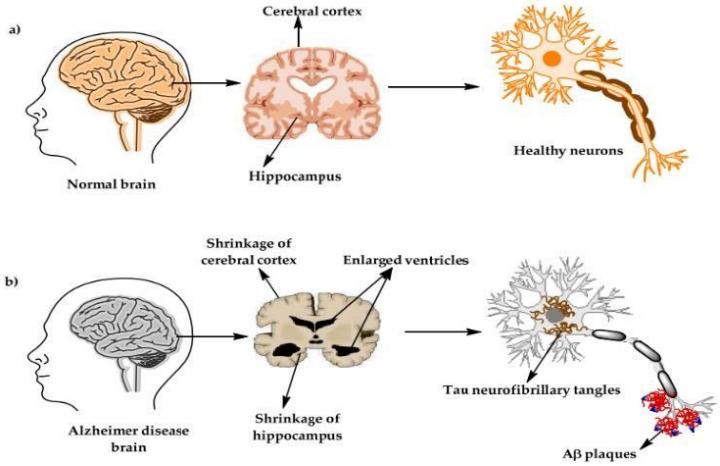

Figure 1 - ***The physiological and pathological (AD) structure of the brain and neurons****. (a) Healthy brain and (b) Alzheimer's disease (AD) brain. Adapted from [4].*

The progression of AD from unnoticeable brain changes to memory loss and later physical disability is called the AD continuum. The AD continuum has 3 main phases: (1) preclinical AD, which due to the absence of symptoms can be referred as healthy control (HC) ornormal control (NC); (2) Mild cognitive impairment (MCI), the intermediate phase in which the progression is more rigorously observed for diagnosis of AD pathology or not; and finally (3) AD,which is the final phase and is divided into stages that reflect the degree to which the symptomsinterfere with the ability to perform daily tasks- with mild, moderate and severe stages. The duration of each phase varies and is influenced by age, gender, genetics and other factors [5].

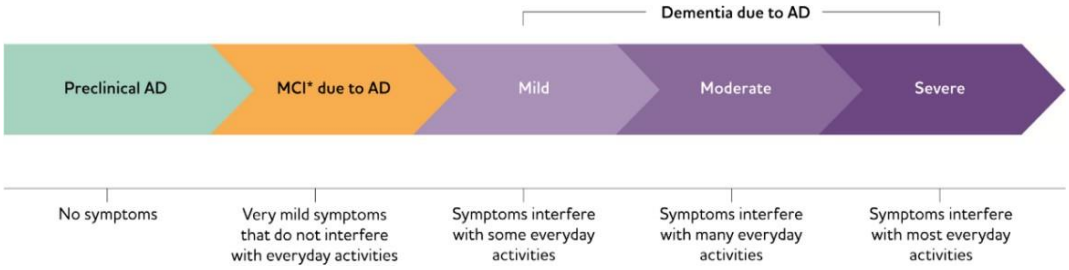

*Figure 2 - **AD continuum**. Scale of symptom impacts. From [5].*

In 2018, Alzheimer's Disease International estimated a dementia prevalence of about 50 million people worldwide, projected to triple in 2050 [2].

According to a multicenter study that provided estimates of duration of the stage of dementia, prodromal (mild cognitive impairment) and the preclinical disease stage of Alzheimer's disease, for an individual aged 70, estimates that the duration are 10 years for the preclinical internship, 4 years for the prodromal internship, and 6 years for the dementia of Alzheimer's disease, totaling 20 years [2].

In addition, women are more likely to develop AD than men, especially after 80 years of age, because they are more likely to have a higher Tau load, although they have a similar amyloid β burden [2]. In addition, cardiovascular risk factors and a harmful lifestyle were associated with an increased risk of dementia [2].

The autosomal dominant inherited AD (DIAD) form affects less than 1% of patients. This is characterized by an early age of disease onset (~45 years), however, the disease is only confirmed post mortem by observation of Aβ and neurofibrillary tangles in the brain. The diagnosisof AD is based on clinical observations and cognitive tests such as neuropsychological tests [6].

1.2. Tau Isoforms, Structure and Function

Tau protein is part of the microtubule-associated proteins (MAP) family. Human Tau protein is encoded by the microtubule-associated protein Tau (MAPT) gene located on the long arm of chromosome 17 (17q21). It has 16 exons, whose alternative splicing generates multiple Tau isoforms [7, 8, 9].

This alternative splicing of the MAPT gene from exons 2, 3, and 10 results in six isoforms of Tau, composed of 352 to 441 amino acid residues with an approximate molecular weight of 36.8 to 45.9 kDa. These isoforms differ by containing zero (0N), one (1N) or two (2N) amino

terminal inserts (29 amino acids each, encoded by exons 2 and 3); and also three (3R Tau) or four (4R Tau) repeats (31-32 amino acids) in the microtubule-binding domain (MTBR) encoded by exon 10. In summary, Tau has six isoforms: 0N3R, 1N3R, 2N3R, 0N4R, 1N4R, and 2N4R [7, 8, 10].

The 0N3R Tau isoform is the smallest and lacks the extra repeat in the MTBR and both amino-terminal inserts, containing 352 amino acids residues (hTau352). This is the only isoform expressed in the fetal human brain [8].

The longest human Tau isoform expressed in the brain is the 2N4R, containing a total of 441 amino acids residues (hTau441). It is composed of 56 negative residues (asparagine or glutamine), 58 positive residues (lysine or arginine), 80 serine or threonine residues, and 8 aromatic residues (5 tyrosine and 3 phenylalanine, but wiothout tryptophan) [8].

The levels of 3R Tau and 4R Tau forms are roughly equal, and their imbalance affects their microtubule-binding affinity and also their propensity for aggregation, being sufficient to cause neurodegeneration and dementia [8].

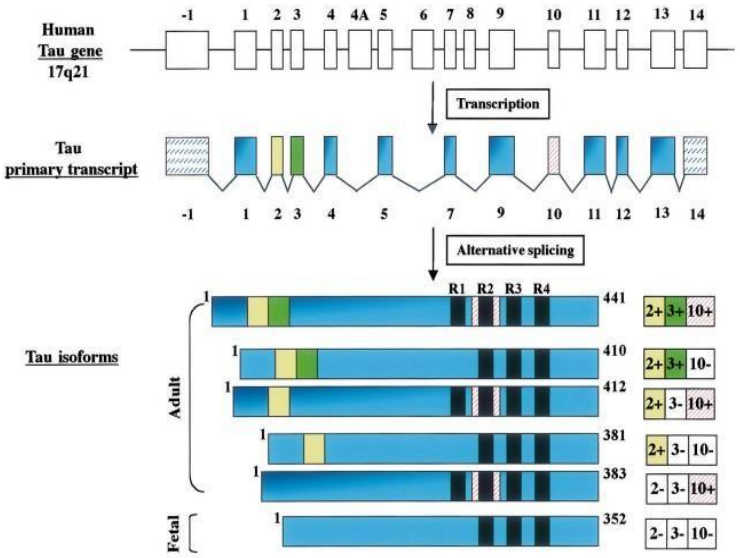

Figure 3 - ***Scheme of the human Tau gene (16 exons), the human Tau primary transcript (13 exons, since exons 4A, 6 and 8 are not transcribed in human) and the six human Tau isoforms****. Exons 1 and 14 are transcribed but not translated. Exons 1, 4, 5, 7, 9, 11, 12, 13 are constitutive. Instead exons 2, 3, and 10 are alternatively spliced. These leads to six different mRNAs. These isoforms differ by the absence or presence of one or two inserts encoded by exon 2 (yellow box) and 3 (green box), in combination with three (R1, R3 and R4) or four (R1–R4) repeats (black boxes) in the MTBR. The fourth microtubule-binding repeat is encoded by exon 10 (slashed box). From [11].*

Tau protein is an intrinsically disordered and highly soluble protein that plays an important role in promoting microtubules stabilization and polymerization[10].

Tau comprises several functional domains. The first is the N-terminal projection domain that regulates microtubule binding even though it is not directly involved in the physical interaction, and this domain consists of residues 1–150 (for the longest isoform). Then, there is the proline-

rich domain that represents the most disordered part of the protein. This domain serves as an interaction site for Src homology-3 (SH3) proteins, and also for RNA and DNA. The proline-rich domain is located in the central portion of Tau from residue 151–243. And finally, the microtubule-binding repeat domains (MTBR) that interact with microtubules and also with actin [12].

The assessment of Tau's structure has been highly challenging due to its disordered features. Moreover, the progress in understanding Tauopathies in general has been hindered by the lack of atomic structures of Tau from brain samples.

1.3. Tau Hyperphosphorylation

Tau hyperphosphorylation strongly modulates Tau functions and is associated with Tauopathies. There are currently 85 known phosphorylation sites on Tau, including 45 serine, 35 threonine, and five tyrosine residues, which comprise 53, 41, and 6% of the residues that can be phosphorylated on Tau, respectively [7].

Tau phosphorylation plays a critical role because it regulates Tau's affinity for microtubules. This protein is physiologically constantly phosphorylated and dephosphorylated to ensure the regulation of proper functions. Its phosphorylation status is the result of a tightly regulated balance of actions between many cellular proteins: mainly kinases and phosphatases that phosphorylate and dephosphorylate it, respectively. When the balance of Tau's phosphorylation state is shifted towards phosphorylation (hyperphosphorylated Tau), its affinity for microtubules decreases resulting in cytoskeleton destabilization, particularly in neurons, and an increase in cytosolic Tau, thus becoming more prone to aggregation [8].

Tau kinases are divided into three different groups, the first being proline-directed serine/threonine kinases, such as glycogen synthase kinase (GSK3), cyclin-dependent kinase-5 (CdK5), mitogen-activated protein kinases (MAPKs), and other kinases that are activated by stress. The second group is non-proline driven serine/threonine kinases, including dual-specificity regulated tyrosine phosphorylation kinase 1A (DYRK1A), cAMP-dependent protein kinase A (PKA), calcium/calmodulin-dependent protein kinase II (CaMKII) and casein kinase 1 (CK1). Finally, the third group is tyrosine kinases such as Fyn and Src [8, 13].

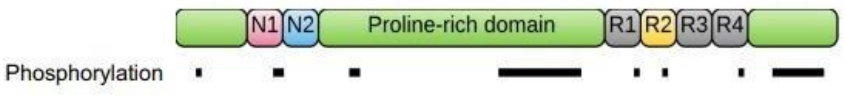

Figure 4 - ***Post-translational modification of Tau.*** *Illustration of the phosphorylation sites on Tau. The black barsindicate the approximate sites for phosphorylation on the 2N4R Tau isoform. From [13]*

When hyperphosphorylated, the Tau protein undergoes conformational changes, namely its monomer forms a dimer and subsequently an oligomer, that acquires a more ordered β-sheet structure. This induces aggregation in paired helical filaments and consequently, forming neurofibrillary tangles [8, 13].

1.4. Tau mutations

Several disease-mutations were already identified in the MAPT gene; until January 2017 fifty-nine pathogenic MAPT mutations were identified [14]. These mutations in the MAPT gene give rise to several different clinical phenotypes, most of which are frontotemporal dementia (FTD), but which also include Parkinson's disease (PD) progressive supranuclear palsy (PSP), Lewy body dementia (LBD), Pick's disease (PiD), argyrophilic grain disease (AGD) and FTD/amyotrophic lateral sclerosis (ALS) [13].

The first mutation identified in the MAPT gene that resulted in Tau dysfunction and neuronal death was the P301L mutation. Later, many other mutations were discovered, one of which affects the ratio of 3R and 4R isoforms, increasing Tau phosphorylation. Since the 4R isoforms have a greater propensity to bind to microtubules, this binding can be significantly affected by the presence of these mutations [8, 13].

The influence of specific disease-associated mutations in the Tau protein on microtubule binding is one of the functions established, but there are others not well established. However, it is clear that MAPT mutations are detrimental to neurons and possibly impact the Tau conformation resulting in post-translational modifications, interaction with other proteins, and other intracellular processes [13].

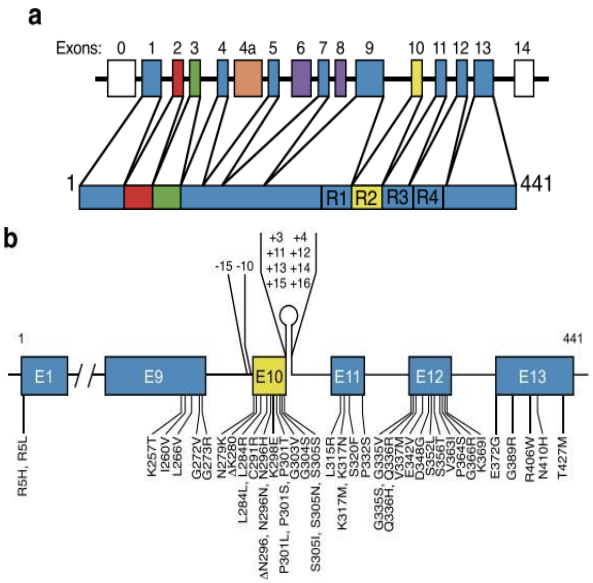

Figure 5 - Representation of MAPT mutations and Tau isoforms. *a - exons 0-16 of MAPT; Red, yellow and green - Alternative mRNA splicing that gives to six Tau isoforms; Blue - constitutively spliced exons.White - noncoding 0 and E14; Violet - E6 and E8 not transcribed in human brain; Orange - only expressed in the peripheral nervous system; R1, R2, R3 and R4 - repeat domains. b - Frontotemporal dementia examples of mutations in MAPT; Are shown 10 intronic mutations flanking E10 and 49 coding region mutations. From [14].*

MAPT mutations are centered on exons 9-12 (encode R1-R4) and the introns that flank exon 10. These mutations can affect the protein level or the alternative splicing of Tau pre-mRNA. (Fig 5). Mutations acting at the protein level can delete or alter single amino acids, resulting in a reduced ability of the protein to interact with microtubules. The mutations that act at the RNA level are intronic or exonic and result in an increase in the alternative splicing of the exon 10 mRNA, affecting the proportion of the 3R and 4R isoforms, the latter being relatively overproduced and resulting in its assembly into aggregates [14].

1.4.1. P301L Mutation

The P301L Tau mutation is a critical genetic variant associated with neurodegenerative diseases, particularly frontotemporal dementia (FTD) and various Tauopathies. This specific mutation located in exon 10, results in a substitution of a proline (P) amino acid for leucine (L) at position 301 of the Tau protein and has no effect on the alternative splicing of exon 10 (table 1) [15, 16].

P301L Tau has the lowest potential to promote microtubule- assembly and the greatest tendency to form Tau filament. The P301L Tau mutation disrupts the ability of Tau to bind and stabilize microtubules. As a result, Tau molecules detach from microtubules more easily and tend

to aggregate into toxic clumps within neurons. These Tau aggregates, or tangles, are a hallmark of tauopathies and are strongly linked to neuronal dysfunction and cell death [15, 16, 17].

Frontotemporal dementia associated with the P301L Tau mutation is characterized by the degeneration of neurons in the frontal and temporal lobes of the brain. This leads to progressive cognitive and behavioral impairments, including changes in personality, language difficulties, and memory problems [5].

*Table 1 – **The amino acid sequencPOPCes of WT 2N4R Tau and P301L Tau protein. Blue** – N-terminal and C-terminal;**Yellow** – proline-rich region; **Green** – microtubule-binding domain; **Orange** – the mutation at position 301 (substitution of a proline (P) amino acid for leucine (L)).*

Sequence
WT 2N4R Tau
MAEPRQEFEV MEDHAGTYGL GDRKDQGGYT MHQDQEGDTD AGLKESPLQT PTEDGSEEPG SETSDAKSTP TAEDVTAPLV DEGAPGKQAA AQPHTEIPEG TTAEEAGIGD TPSLEDEAAG HVTQARMVSK SKDGTGSDDK KAKGADGKTK IATPRGAAPP GQKGQANATR IPAKTPPAPK TPPSSGEPPK SGDRSGYSSP GSPGTPGSRS RTPSLPTPPT REPKKVAVVR TPPKSPSSAK SRLQTAPVPM PDLKNVKSKI GSTENLKHQP GGGKVQIINK KLDLSNVQSK CGSKDNIKHV PGGGSVQIVY KPVDLSKVTS KCGSLGNIHH KPGGGQVEV SEKLDFKDRV QSKIGSLDNI THVPGGGNKK IETHKLTFRE NAKAKTDHGA EIVYKSPVVS GDTSPRHLSN VSSTGSIDMV DSPQLATLAD EVSASLAKQG L
P301L 2N4R Tau
MAEPRQEFEV MEDHAGTYGL GDRKDQGGYT MHQDQEGDTD AGLKESPLQT PTEDGSEEPG SETSDAKSTP TAEDVTAPLV DEGAPGKQAA AQPHTEIPEG TTAEEAGIGD TPSLEDEAAG HVTQARMVSK SKDGTGSDDK KAKGADGKTK IATPRGAAPP GQKGQANATR IPAKTPPAPK TPPSSGEPPK SGDRSGYSSP GSPGTPGSRS RTPSLPTPPT REPKKVAVVR TPPKSPSSAK SRLQTAPVPM PDLKNVKSKI GSTENLKHQP GGGKVQIINK KLDLSNVQSK CGSKDNIKHV LGGGSVQIVY KPVDLSKVTS KCGSLGNIHH KPGGGQVEV SEKLDFKDRV QSKIGSLDNI THVPGGGNKK IETHKLTFRE NAKAKTDHGA EIVYKSPVVS GDTSPRHLSN VSSTGSIDMV DSPQLATLAD EVSASLAKQG L

1.5. Tau Neurotoxicity

Tau protein has been found to have harmful effects on the genome of neurons. Tau protein can enter the nucleus of neurons and form protein-DNA complexes, which can interfere with the normal functioning of DNA. Tau protein has also been shown to interact with specific regions of DNA in the chromosome, which are important for maintaining genomic stability. Dysfunctional nuclear Tau has been linked to DNA damage and impaired DNA repair mechanisms, which can lead to genomic instability and neuronal dysfunction. Additionally, Tau protein plays a role in protecting RNA and DNA from damage induced by oxidative stress and in sustaining the dense chromatin structure. Dysfunctional Tau can impair these protective mechanisms, leading to further DNA damage and neuronal dysfunction. These harmful effects of Tau on the genome of neurons may contribute to the development of neurodegenerative diseases such as AD [18].

Tau protein has been discovered to disrupt the functioning of mitochondria, impairing energy production in neurons. Mitochondria are cell organelles responsible for generating ATP, the cellular energy currency. When Tau protein interferes with normal mitochondrial processes, it hampers ATP production and triggers an increase in the production of reactive oxygen species (ROS). This oxidative stress damages neurons, leading to dysfunction and eventual cell death. Moreover, Tau protein also disrupts the regulation of lipid and calcium metabolism, which are crucial for maintaining mitochondrial function. These disturbances in mitochondrial function and energy production are also strongly associated with AD [18].

Tau oligomers specifically affect synaptic integrity and function in neurons. Some studies showed that Tau oligomers diminish the number of synapses and reduce the levels of synaptic vesicle-bound proteins. Additionally, Tau oligomers disrupt the trafficking of synaptic vesicles, which is vital for proper synaptic function. These effects on synaptic integrity and function closely resemble the changes observed in AD and other tauopathies. Furthermore, Tau oligomers induce alterations similar to those seen in AD, such as increased basal GABA release and decreased glutamate receptors. Notably, these effects are not observed when Tau monomers are present, indicating that Tau oligomers selectively impact synaptic integrity and function [18].

Tau oligomers negatively impact microtubule assembly, neuronal cytoskeleton, and axonal transport. Microtubules play a crucial role in maintaining neuronal shape and facilitating the transport of organelles and cellular components. While Tau protein normally stabilizes microtubules, Tau oligomers interfere with this process, resulting in microtubule instability. Consequently, the neuronal cytoskeleton and axonal transport are disrupted, leading to neuronal dysfunction and death. Furthermore, Tau oligomers impair the axonal transport of various organelles, including peroxisomes, neurofilaments, Golgi-derived vesicles, neurotrophin receptors, and amyloid precursor protein (APP). The disruption of organelle transport within neurites poses a significant risk to neurons, potentially causing their degeneration and death. Notably, Tau inhibits the transport of mitochondria into axons and dendrites, which severely compromises energy production in regions with high energy demands, such as synaptic connections [18].

Defective protein degradation is a common feature of many neurodegenerative diseases, including AD and other Tauopathies. The accumulation of toxic or inactive proteins within neurons can result in malfunction, degeneration, and ultimately cell death. Proper maintenance of intracellular protein levels and states (known as proteostasis) is essential for cellular function. Proteostasis is achieved through continuous protein synthesis and the restoration or degradation of proteins, facilitated by a complex cellular machinery called protein quality control. If these processes fail, the accumulation of toxic or inactive proteins occurs, leading to malfunction, degeneration, and eventual cell death. Imperfect proteostasis, particularly compromised Tau turnover, is implicated in various diseases, including tauopathies, with AD being the most prominent. In AD, Tau protein accumulates as neurofibrillary tangles, which are considered neurotoxic and believed to be a causative factor in the disease [18].

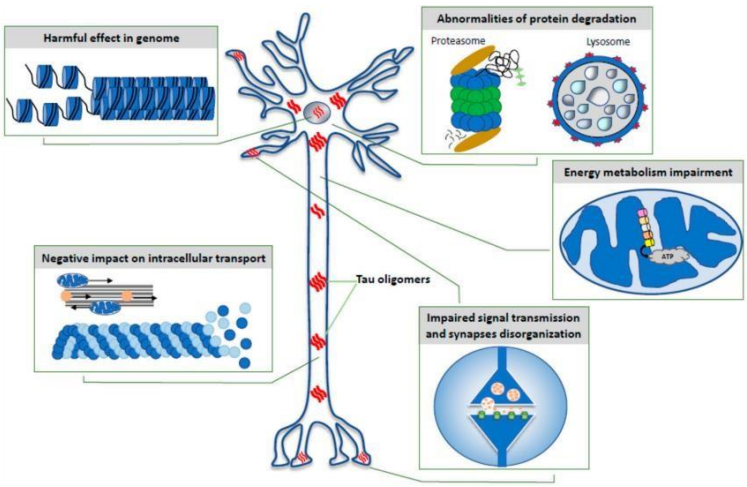

Figure 6 - ***Schematic illustration of intraneuronal processes affected by the formation of toxic Tau oligomers****. From [18].*

1.6. Pathology of Tau in Alzheimer's Disease

The presence of Aβ (Beta-amyloid) leads to the hyperphosphorylation of Tau protein and subsequently to the generation of clusters, resulting in diseases such as inflammation, formation of Tau tangles, dysfunction of synapses, and cell death [19]. The Phosphorylation of Tau proteinis associated with the destabilization of microtubules (loss-of-function) and the assembly of Tauprotein into higher order aggregates (gain of function) [19].

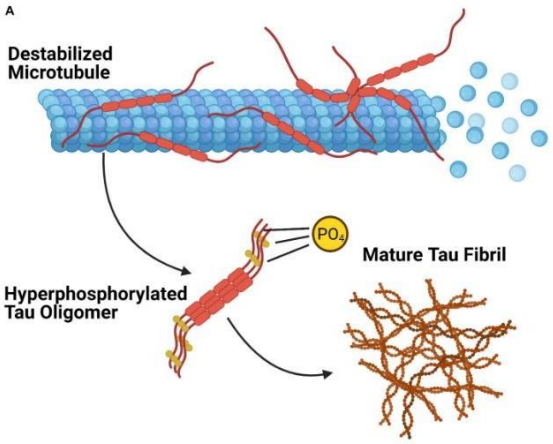

Figure 7 - ***The Pathological Deposition of Tau Protein in AD.*** *From [19].*

1.6.1. Tau amyloid aggregation

Tau aggregation is a defining feature of several neurodegenerative disorders and is also observed as a natural occurrence in aging brains with Tau aggregates. The process of Tau aggregation, considering its native disordered unfolded state, highly structured aggregates, and periodic fibrils, is expected to have a low probability of happening. However, two short hexapeptide motifs, VQIINK and VQIVYK, located at the beginning of R2 and R3 regions, respectively, have a tendency to form β-sheet structures and play a crucial role in Tau aggregation [20]. Even partial involvement of these sequences can initiate aggregation. The VQIVYK motif alone has been shown to be sufficient for fibril formation with interdigitated β-sheets, and the onset of Tau aggregation seems to involve the unmasking of this motif, which allows β-sheet stacking. Disruption of these motifs prevents Tau aggregation, while enhancing β-structure formation in these same motifs promotes aggregation [21]. When Tau is bound to microtubules, it doesn't adopt a globular structure but can form local hairpin conformations with residues containing the hexapeptide motifs. This suggests that stabilization of the microtubule-bound Tau conformation delays aggregation [22].

Tau aggregation can be accelerated by inducers such as polyanions, which compensate for the repulsive positive charges of Tau. Heparin is a commonly used inducer *in vitro*, as it stabilizes an aggregation-prone conformation of Tau [23]. Post-translational modifications, particularly phosphorylation, also influence Tau's propensity to aggregate. Hyperphosphorylation precedes Tau aggregation in AD patients and other Tauopathies [24]. However, *in vitro*, Tau aggregation can be induced efficiently by polyanionic cofactors regardless of phosphorylation.

Truncated Tau fragments containing the repeat domain have a higher tendency to aggregate, likely due to the disruption of Tau's "paperclip" structure. These truncations can induce neurodegeneration independently of Tau aggregation.

In vitro studies suggest that Tau aggregation follows a nucleation-elongation mechanism. External seeds from preformed paired helical filaments (PHFs) can accelerate the overall assembly by circumventing the nucleation rate-limiting step [20]. Similar to other amyloid diseases, Tau proteins undergo aggregation via conformational changes, resulting in highly ordered cross-β-sheet structures formed by stacked β-sheet segments. The observed cellular toxicity of Tau is associated with the self-assembly process where free Tau monomers convert into Tau amyloid fibrils. Therefore, it is crucial to understand the molecular events underlying the amyloid formation process, which can be monitored in vitro using thioflavin-T (ThT) fluorescence. ThT fluorescence increases when it binds to cross-β-sheet structures and is excited at 440nm.

In vitro, the formation of fibrils typically follows a sigmoidal growth curve, as depicted in Figure 8. The process begins with a lag phase, also known as the nucleation phase. During this phase, protein monomers, such as Tau, organize into multimers and oligomers that do not exhibit any ThT reactivity, indicating the absence of formed fibril structures. Following the lag phase and

preceding the growth phase, prefibrillar assemblies emerge, displaying cross-β-sheet structures. In the growth phase, monomers continue to be added to the existing protofilaments and protofibrils, leading to exponential fibril growth. Eventually, the reaction reaches a plateau phase, representing the equilibrium state where all monomeric protein has been depleted. This endpoint is determined by the exhaustion of monomers and the establishment of equilibrium in the system [25,26].

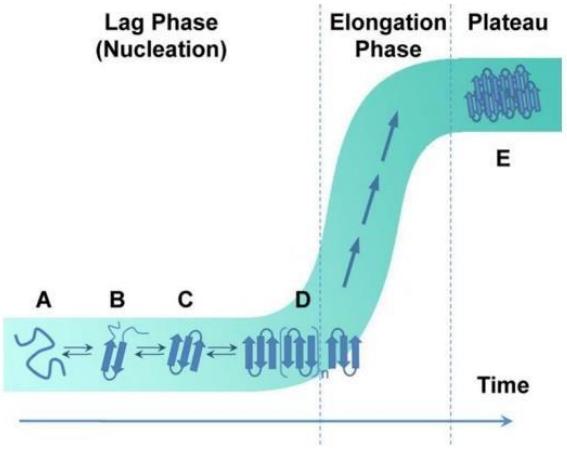

Figure 8 - ***Scheme of formation of fibrils represented as a sigmoidal curve****. Begins with a lag phase when soluble, monomeric, or natively unfolded proteins (A) form β-structures (B), which aggregate to generate the initial nucleus (C) and protofibrils (D). Following with a fast elongation phase, in which monomers and higher order oligomers elongate the nucleus into mature fibrils at the plateau (E). From [26].*

1.6.2. Seeding and Spreading of Tau Proteins

Currently, there is evidence of some factors that determine the pattern of Tau spreading, such as neuronal and regional connectivity, neuronal vulnerability (inadequate myelination and vulnerability to toxins, among others) and processes independent of Tau transmission.

There is still no certainty about which species of Tau are transmitted between neurons and what are the underlying transmission mechanisms. It is known that presynaptic Tau seeds can diffuse across a synaptic cleft as a result of degeneration of presynaptic neurons, causing membrane leakage. Thus, we can have transfer of pathological Tau protein by several mechanisms. One of the mechanisms is direct secretion through the plasmatic membrane, in which there is a cluster of Tau next to it and by interaction with specific lipids (as microdomains of rich in cholesterol/sphingomyelin), resulting in penetration through the membrane and its release (Fig. 9 mechanism 1). Another mechanism is the secretion in ectosomes released from the plasmatic membrane which, after their release from the cell, are fused or endocytosed by the target cell (Fig. 9 mechanism 2). Tau can also be secreted by exosomes, after its release from the cell (its process is very similar to that of ectosomes) and they are also fused or endocytosed by target cells (Fig. 9 mechanism 3). Finally, there may be cell-to-cell transfer through nanotubes that directly connect the cytosol of the cell with the target cell (Fig. 9 mechanism 4) [8].

Despite all possible transfer mechanisms, aggregated Tau reaches the target cell cytosol, allowing the patterned seeding of healthy Tau molecules into pathological misfolded conformations. In turn, target cells can spread the pathology to other cells that are not yet affected [8].

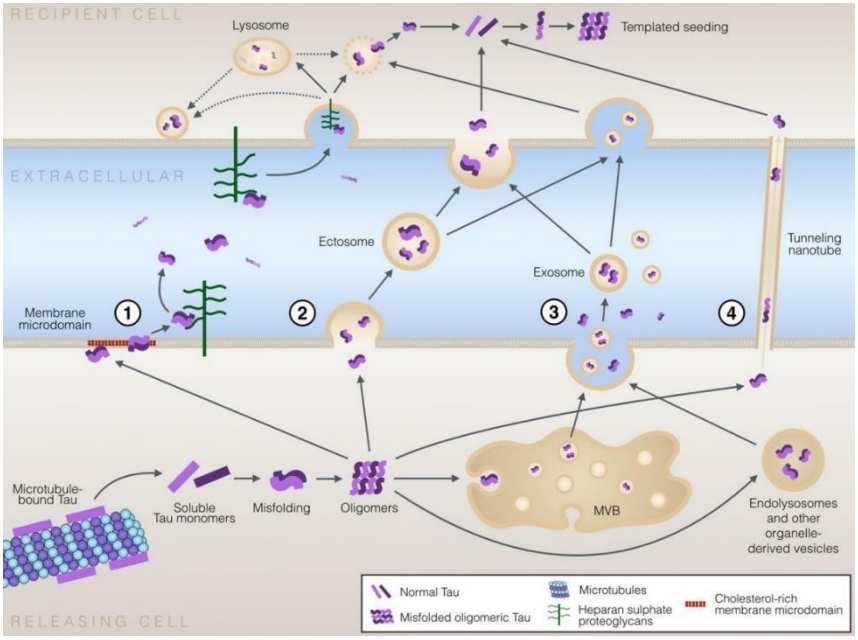

*Figure 9 - **Mechanisms of cell-to-cell transfer of pathological Tau protein**. 1) Direct secretion through the plasmatic membrane; 2) Ectosomes; 3) Exosomes; 4) Cell-to-cell transfer through nanotubes. From [8].*

1.7. Techniques

1.7.1. Fluorescence spectroscopy

Fluorescence spectroscopy stands out as a contemporary and powerful approach to investigate protein folding/dynamics, assembly, interactions and even membrane architecture. It has emerged as an powerful tool, unraveling the intricate mechanisms underlying protein aggregation, including the formation of amyloid fibrils, while shedding light on their ever-changing structural dynamics [27].

Proteins contain intrinsic fluorophores, such as tyrosine, phenylalanine and tryptophan residues, each possessing an innate ability to fluoresce. This intrinsic fluorescence allows to monitor conformational changes of proteins (by exposure or masking of solvents), but proteins can be engineered for introducing fluorescent proteins or even further labelling with small organic dyes [27].

Thioflavin-T (ThT) has been widely used as a non-covalent extrinsic dye for monitoring amyloid fibril formation. It has already gained prominence as a potent fluorescent marker for amyloid structures in histology, due to its selective localization for amyloid deposits [28]. When located in amyloid clusters, ThT exhibits an increased fluorescence signal. This phenomenon arises from the orderly arrangement of ThT molecules that bind to the fibrils, lining up parallel to the long axis of the fiber. This alignment is facilitated by the intricate cross-β-sheet architecture, which effectively "locks" the bound dye, leaving it unable to rotate, thereby enhancing ThT fluorescence intensity [29, 30].

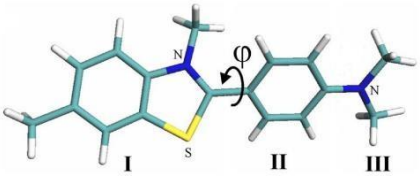

Figure 10 - ***Model of thioflavin T molecule****. From [31].*

This dye exhibits broad applicability to all proteins that give rise to amyloid fibrils, regardless of their unique amino acid sequences. Their interaction is remarkably specific,inducing a substantial change in both excitation maximum (from 385 to 450 nm) and emission maximum (from 445 to 482 nm) [28]. Notably, the fluorescence generated by ThT originates exclusively from its binding to amyloid structures. The substantial increase in ThT fluorescence intensity after binding to fibrils can reach several orders of magnitude, 10-500 times [27].

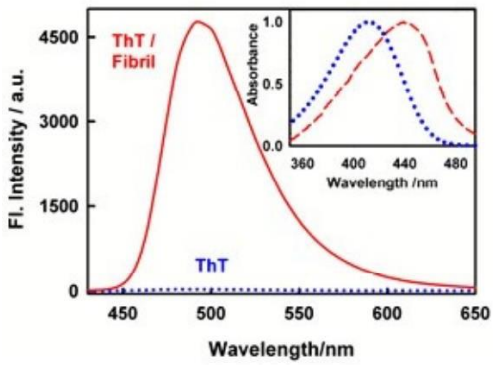

Figure 11 - ***Steady-state emission fluorescence spectrum of ThT in aqueous solution (dotted blue) and in insulin amyloid fibril (solid red).*** *Inset: Normalized absorption spectra of ThT in water (dotted blue) and insulin amyloid fibrils (dashed red). From [32].*

1.7.2. Other Methods to Characterize Fibrillar Structures

Several methods have been employed for studying amyloid fibril. One of the methods used is transmission electron microscopy (TEM), which allows direct visualization of fibrillar structures, providing detailed information about their size, shape and morphology (Fig. 12) [33].

Atomic force microscopy (AFM) is also other technique used that can provide high-resolution topographic images of fibrillar structures and thus measure mechanical properties, such as stiffness and height (Fig. 12) [33, 34]. Another method is circular dichroism (CD) spectroscopy, which can be used to reveal information about the secondary structure of fibrillar proteins [35]. Also widely used is the cryo-electron microscopy (Cryo-EM) method, which provides high-resolution 3D structures of fibrillar aggregates at cryogenic temperatures and is a very valuable method for studying large and complex structures [34]. Other methods such as Fourier transform infrared spectroscopy (FTIR) and solid-state nuclear magnetic resonance (NMR) can also be used in the study and characterization of fibrillar structures, the first being more focused on the secondary structure and composition of fibrils, and the second for structure and interactions within the fibrils [36].

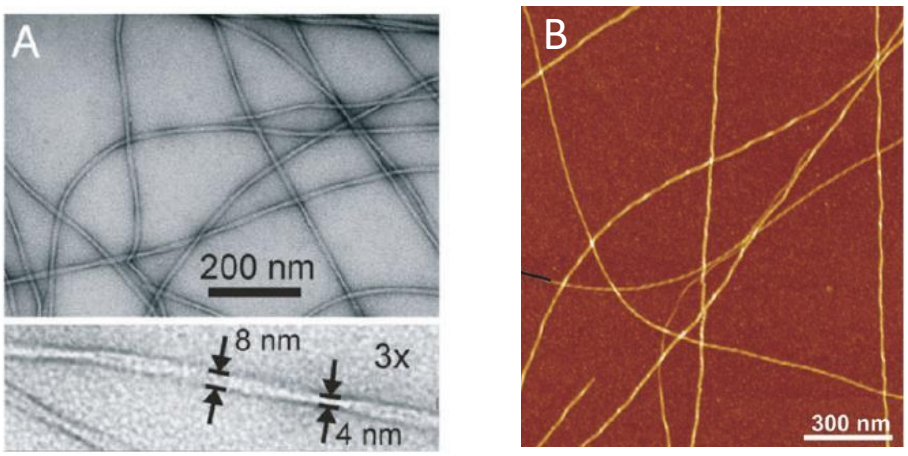

Figure 12 – ***Examples of two methods for characterizing fibrillar structures. TEM and AFM. A -*** *Negatively stained TEM image of Aβ (1–40) fibrils.* ***B -*** *AFM height image of β-lactoglobulin fibrils obtained after heating at pH 2 for 5 h at 90 °C. Adapted from [33].*

1.8. Goals and experimental strategy

The abnormal aggregation of the microtubule-biding Tau protein into neurofibrillary tangles in neurons is a hallmark of numerous neurodegenerative disorders, termed as Tauopathies [3, 4]. Several mutations in Tau (including P301L) associated with these Tauopathies disrupt the ability of Tau to bind and stabilize microtubules and also trigger its aggregation. While most studies have focused so far in the K18 Tau fragment (only with MTBR), here we investigated the fibrillation of the lost Tau isoform (2N4R Tau), both WT and P301L mutation, in the presence of two aggregation- inducers, such as heparin and anionic lipid membranes.

The thesis was organized in two major work plans:

- Expression and purification of WT and P301L 2N4R Tau protein. For P301L mutation, the original plasmid was engineered for expression of Tau with the P301L mutation by site-directed-mutagenesis.
- ThT fluorescence assays for monitoring the fibrillation of WT and P301L 2N4R Tau in solution and in the presence of heparin (0.5 mg/mL and 1.0 mg/mL) and anionic lipid vesicles (50:50 1-palmitoyl-2-oleoyl-*sn*-glycero-3-phosphocholine (POPC) : 1-palmitoyl-2-oleoyl-*sn*-glycero-3-phospho-L-serine (POPS), 25 µM, 50 µM and 100 µM).

2. Materials and Methods

2.1. Plasmids, Bacterial cells, Chemicals and Materials

The plasmid pET-HT-Tau for expressing the full-length 2N4R Tau with a cleavable His-tag was a gift from Professor Elizabeth Rhoades (University of Pennsylvania, USA) [37]. pRK793 plasmid for producing His_6-Tobacco Etch Virus (TEV) was a gift from David Waugh (Addgene plasmid # 8827) [38].

All chemicals, materials and bacterial strains used and their respective providers are detailed in Table 2.

Table 2 – List of all materials, chemicals and bacterial cells used with their respective providers.

Material, chemicals and bacterial cells	**Manufacturer**
1-palmitoyl-2-oleoyl-glycero-3-phosphocholine (POPC)	Avanti Polar Lipids
1-palmitoyl-2-oleoyl-*sn*-glycero-3-phospho-L-serine (POPS)	
E. coli MAX Efficiency™ DH5α	Thermo Fisher Scientific
E. coli One Shot® BL21(DE3) Chemically Competent	
dNTP Set 100 mM solutions	
Pierce™ BCA Protein Assay Kits	
Slide-A-Lyzer™ Dialysis Cassettes of 10 kDa cutoff	
Tris-(2-Carboxyethyl)phosphine, Hydrochloride (TCEP)	
FastDigest DpnI	
Luria Broth (Miller´s LB Broth)	NZYTech
Isopropyl β-D-1-thiogalactopyranoside (IPTG)	
Dithiothreitol (DTT)	
Ampicilin (Amp)	
BlueSafe	
Protein Marker II	
NZYMiniprep Kit for plasmid extraction/purification	
cOmplete Mini EDTA-free Protease Inhibitor Cocktail Tablets	Roche
Phenylmethylsulfonyl fluoride (PMSF)	PanReac AppliChem
Primer forward and reverse for site-directed mutagenesis	Stab Vida
Amicon® Ultra-15 Centrifugal Filters with 3 kDa and 10 kDa cutoff	Millipore
5 mL HisTrap FF columns	.Cytiva Life Sciences
HiLoad™ 16/600, Superdex™ 200 pg column	
0.45 µm syringe filters (low protein binding)	Labbox (SFPE-245-100)
96-well microplates F-bottom and non-binding protein	Greiner Bio-One
ThT	Sigma
Lysozyme from chicken egg white	
Heparin	
PfuUltra High-fidelity DNA Polymerase	Agilent Technologies

Chemicals for buffers to Tau expression/purification, SDS-PAGE and ThT assays were obtained from Sigma and Thermo Ficher Scientific. The buffers were prepared with Milli-Q water, filtered through 0.2 µm membrane filters, and always stored at 4 ºC.

2.2. Site-Directed Mutagenesis

To explore the role of the P301L disease-mutation in Tau aggregation, the pET-HT-Tau plasmid was engineering for introducing a T instead of a C in the codon 301 (CCG to CTT) for expressing P301L 2N4R Tau. This mutation was introduced by the QuikChange II Site-Directed Mutagenesis method (from Agilent) [39].

A PCR-based site-directed mutagenesis was performed in a SimpliAmp Thermal Cycler (Thermo Fisher) and using a reaction mix composed of: (i) 5 µL of 10× PfuUltra HF reaction buffer, (ii) 1 µL of 40 mM of dNTPs mixes, (iii) 1.25 µL of 0.1mg/ml of each primer (for 125 ng), (iv) 1 µL of DNA template (25-35 ng), (v) 1 µL of *PfuUltra* High-Fidelity DNA polymerase and then (vi) water for a total volume of 50 µL. The PCR reaction was initiated by preheating the reaction mixture to95°C for 30 seconds, followed by 16 cycles of 95°C for 30 seconds, 55°C for 1 minute and 68°Cfor 10 minutes, and finally cooled to 4°C.

Table 3 - Sequence of the mutagenesis primers designed using the PrimerX program.

P301L Forward Primer	5' GATAATATCAAACACGTCTTGGGAGGCGGCAGTGTGC 3'
P301L Reverse Primer	5' GCACACTGCCGCCTCCCAAGACGTGTTTGATATTATC 3'

After PCR, 1µL of DpnI was added and incubated at 37°C for 1 hour. Then, 50 µL of *E. coli* DH5α cells were transformed with 4 µL of the previous reaction by the heat shock method. Then, 250 µL of the transformation was spread on LB agar plates containing 100 µg/ml of Amp.

Single colonies were inoculated in 25 mL LB-Amp medium (with 100 µg/ml of Amp) and were then grown overnight (O/N) at 37 ºC with 250 rpm shaking. The plasmid extraction was performed with the NZY Miniprep Kit using the manufacturer's recommended protocol [40]. Subsequently, DNA concentration was assessed using a NanoDrop™ One/One (Thermo Fisher). Sequencing was carried out by Stabvida services using the T7 Terminator and T7 Forward primers (Table 4) to validate the presence of the P301L mutation. Sequence alignment was conducted using the Clustal Omega Alignment Tool (https://www.ebi.ac.uk/Tools/msa/clustalo/).

Table 4 - Sequencing primers.

T7 Forward Primer	5' TAATACGACTCACTATAGGG 3'
T7 Terminator Primer	5' GCTAGTTATTGCTCAGCGG 3'

2.3. Tau Expression and Purification

2.3.1. Tau Expression

E. coli One Shot® BL21(DE3) cells were transformed with the pET-HT-Tau WT or P301L plasmid by heat shock, then spread on a LB-Agar plate with 100 µg/ml Amp, and finally incubated O/N at 37°C. Next, a single colony was inoculated in 25 mL of LB-Amp and incubated O/N at 37°C with 250 rpm shaking. The next morning, the culture was renewed using 10 mL of the O/N inoculum and 90 mL of fresh LB-Amp, and then left to grow for 3 hours under the same conditions.

For evaluating the IPTG concentrations for Tau expression, 1L of LB-Amp medium was inoculated with the previous culture to reach an optical density at 600 nm (OD_{600nm}) = 0.1. The cells were then incubated ate 37°C and 250 rpm until attain an OD_{600nm} between 0.5 and 0.6. Different IPTG concentrations were evaluated for Tau expression: (i) 0 mM, (ii) 0.4 mM, (iii) 0.6 mM, (iv) 0.8 mM and (v) 1 mM. For protein expression, the culture was divided into four different culture flasks (each with 100 mL), IPTG added, and finally the cells were incubated O/N at 16°C with 250 rpm shaking. Samples were taken using a ratio of 1.2/OD, in order to maintain the number of cells, before and after IPTG induction, then centrifuged at 8000 rpm for 2 minutes at 4 ºC, and the pellet was resuspended in 80 µL of loading buffer (50 mM Tris-HCl pH 6.8, 100 mM DTT, 2% sodium dodecyl sulfate (SDS), 0.1% bromophenol blue, and 10% glycerol). Finally, a SDS-PAGE gel was performed to confirm the best IPTG concentration to induce Tau expression. We note that the number of cells must be maintained in all samples, otherwise the band on the SDS-PAGE gel may be more or less intense, depending on whether there are more or fewer cells.

The large-scale expression of Tau protein (WT and P301L 2N4R Tau) was performed in 2 flasks of 1.5L LB-Amp (with the same conditions) at 16 ºC with 250 rpm shaking, and using 0.6 mM of IPTG. The cells were harvested by centrifugation at 6000 rpm for 15 min, and 4 ºC. The cell pellets were stored at -80 ºC until purification.

2.3.2. Tau Purification

Cells (from a total of 3L culture) were resuspended in 60 mL Nickel buffer A (50 mM Tris pH 8, 500 mM NaCl, 10 mM Imidazole) containing 1 mM PMSF, 1 mg/mL lysozyme and 3 tablets of complete Mini EDTA-free Protease Inhibitor Cocktail. Cells were then sonicated on ice in a Branson Sonifier 250, with 10 cycles of 15 pulses (50% duty cycle and an output of 9) and 2 minutes off between cycles. Finally, the cells were centrifugated at 13 000 x*g* for 50 minutes and at 4ºC. After centrifugation, the supernatant was collected and filtered with a 0.45 µM syringe filter (low protein binding).

Then, a first immobilized metal affinity chromatography (IMAC) was performed using a 5 mL HisTrap™ FF column in an ÄKTA™ Start system (GE Healthcare). The filtered lysate was loaded into the column previously equilibrated with Nickel buffer A and with a flow rate of 1.5 mL/min. The non-specific bound proteins were washed out at a flow rate of 5 mL/min of Nickel buffer A with 10 column volumes (CV). His_6-Tau protein was then eluted with a gradient of 0-100% of Nickel buffer B (50 mM Tris-HCl, pH 8.0, 500 mM NaCl, 500 mM Imidazole) at a flow rate of 1.5 mL/min and in 5-mL fractions. The fractions containing the His_6-Tau protein were joined, concentrated and buffer exchanged to Nickel buffer A (to decrease the imidazole concentration) using an Amicon Ultra-15 with a 10 kDa MW cutoff. To cut off the His-tag, half a volume of TEV protease and 1 mM DTT were added and incubated at 4°C in a rotor O/N.

A second IMAC was performed to remove the His_6-tag and TEV protease. The sample was loaded into the 5 mL HisTrapp FF column equilibrated with Nickel buffer A. The Tau protein (without His_6-tag) was initially eluted in the flow-through at a flow rate of 1.5 mL/min and in 2.5 mL fractions. The fractions containing Tau protein were concentrated to a volume of ~2 mL and buffer exchange to buffer C (25 mM Tris pH 8.0, 100 mM NaCl, 1 mM EDTA and 0.5 mM TCEP. in an Amicon.

Finally, a size exclusion chromatography (SEC) was performed for final purification with HiLoad 16/600 Superdex 200 column equilibrated with buffer C, at a flow rate of 0.5 mL/min and fractions of 2 mL were collected. Fractions containing pure Tau protein were aliquoted (in 150 µL) in Eppendorf low protein binding tubes and finally flash-frozen in liquid nitrogen for storage at -80ºC.

The protein concentration was quantified by the Pierce BCA Protein Assay Kit (from Thermo Fisher Scientific) using the microplate procedure and also by absorbance at 280 nm in a NanoDrop™ One/One (Thermo Fisher) [41]. The concentration was then calculated with the molecular extinction coefficient of Tau: 7450 M^{-1} cm^{-1} [42].

2.4. Expression and Purification of TEV protease

The TEV protease was expressed in *E. coli* BL21(DE3) cells. Briefly, these cells were transformed with the pRK793 plasmid and then an O/N inoculum was prepared as detailed for Tau protein. Then, 1 L of fresh LB-Amp medium was inoculated with the previous O/N culture for an OD_{600nm} of 0.1. The culture was grown at 37°C with 250 rpm shaking until reach an OD_{600nm} of ~0.5 and then TEV expression was induced with 1 mM IPTG. The culture was further incubated at 37°C with 250 rpm shaking for 4 hours. Samples for SDS-PAGE analysis were collected both before and after IPTG induction. The cells were then centrifuged at 6000 rpm for 15 min, and 4 ºC. The cell pellets were resuspended in buffer A_{TEV} (50 mM sodium phosphate pH 8.0, 200 mM NaCl, 25 mM imidazole, 10% glycerol) and then stored at -80°C.

Cells were lysed and the cell debris removed as outlined for Tau protein (Section 2.2.1). The TEV protease contains a His_6-tag and therefore was purified by IMAC. Briefly, the filtered supernatant was loaded into a 5 mL HisTrap column at a flow rate of 1.5 mL/min. To remove non-specifically bound proteins, the buffer A_{TEV} was passed through the column at a flow rate of 5 mL/min with 10 CV. Subsequently, TEV protease was eluted using a linear gradient ranging from 0% to 100% of buffer B_{TEV} (50 mM sodium phosphate pH 8, 200 mM NaCl, 250 mM imidazole, 10% glycerol). The fractions were analysed by SDS-PAGE. Those fractions containing the TEV protease were combined and their concentration was quantified by measure the absorbance at 280 nm in a NanoDrop™ One/One (Thermo Fisher). The concentration was then calculated with the molecular extinction coefficient of Tau: 7450 M−1 cm−1 [42].

Next, the selected fractions (~25mL) were dialyzed O/N at 4ºC using a Slide-A-Lyzer™ Dialysis Cassettes (10 kDa cutoff) against buffer $TEV_{storage}$ (50 mM Tris pH 7.4, 1 mM TCEP, and 50% glycerol) and finally stored in 400 µL aliquots at -80ºC

2.5. SDS-PAGE

Samples before and after IPTG induction and between each purification step were analysed by SDS-PAGE gel. We used gels composed of 15% polyacrylamide (for resolving) and also containing 5% polyacrylamide (for stacking). 20 µL sample was mixed with 10 µL of loading buffer. Electrophoresis was initially performed at 80 V for 10 minutes and then at 120 V for 50 minutes in a Mini PROTEAN Tetra Cell system (Bio-Rad). The gels were stained with BlueSafe.

2.6. Liposome Preparation

Large unilamellar vesicles (LUVs) with a mixture of 50:50 of POPC (zwitterionic lipid) and POPS (anionic lipid) were prepared as an anionic aggregation-inducer of Tau protein. The

concentrations of the stock lipid solutions were measured using the phosphate analysis adapted from [43].

The stock solutions of POPS and POPC (in chloroform) were combined for a final lipid concentration of 1 mM. The solvent was then evaporated using a stream of nitrogen and also under vacuum for 3 hours. The lipid film was resuspended in 50 mM Tris pH 7.4, 1 mM DTT, and 50 mM NaCl (buffer for ThT fluorescence assays) and then followed by 10 cycles of freeze-thaw to obtain multilamellar vesicles (MLVs). Then the suspension was extruded 31 times through a 100-nm pore diameter polycarbonate membrane in an Avanti Mini-Extruder system to obtain LUVs (extruder assembled according to the manufacturer instructions). Finally, LUVs were stored at 4ºC.

2.7. ThT fluorescence assays

Tau fibrillation was monitored by ThT fluorescence assays performed in a microplate fluorimeter (PolarStar Optima microplate reader, BMG Labtech). We used 96-well microplates F-bottom and non-binding protein with a sealing film on the top of the wells to prevent evaporation. Samples (total volume of 300 µL) were measured every 20 min for 7 days at 37 ºC with an orbital shaking of 150 rpm for 20 seconds before each measurement, using 20 flashes per well and bottom reading. The ThT fluorescence was recorded with an excitation of 440-10 nm and an emission of 480-10 nm.

For aggregation in solution, WT 2N4R Tau (10 µM, 20 µM and 22.8 µM) or P301L 2N4R Tau (20 µM) were incubated with 50 µM ThT in 50 mM Tris pH 7.4, 1 mM DTT, and 50 mM NaCl buffer. For aggregation with heparin, WT 2N4R Tau (20 µM and 22.8 µM) and P301L 2N4R Tau (20 µM) was incubated with 50 µM ThT and 0.5 mg/ml or 1 mg/ml of heparin in the same buffer. For aggregation with anionic LUVs, WT 2N4R Tau (20 µM) and P301L 2N4R Tau (20 µM) were incubated with 50 µM ThT and also 50:50 POPC:POPS LUVs (25 µM, 50 µM and 100 µM) in the same buffer. Several controls were performed: (i) only ThT in buffer, (ii) Heparin and ThT, and (iii) LUVs and ThT.

The treatment of the data obtained from the assays was performed using Excel (Microsoft Office) and OriginLab software.

3. Results and Discussion

3.1. Expression and Purification of WT 2N4R Tau

3.1.1. Expression Test of WT 2N4R Tau

The recombinant expression of WT 2N4R Tau containing a N-terminal His_6-tag and a TEV cleavage site (DYDIPTT**ENLYFQ|G**S) in *E. Coli* BL21(DE3) cells was initially evaluated by a small-scale expression test. In particular, we explored the Tau expression without IPTG (for auto-induction) and with distinct IPTG concentrations (0.4 mM, 0.6 mM, 0.8 mM and 1 mM) O/N at 16ºC. The SDS-PAGE gels obtained from this assay are displayed in Figure 13. OD_{600mn} were also recorded before and after the induction with IPTG (Table 5).

The SDS-PAGE analysis showed no significant expression of Tau fusion protein in the absence of IPTG, revealing that the auto-induction of Tau expression is not significant under our conditions. Furthermore, with IPTG induction appeared a new band running between 63-75 kDa that corresponds to WT 2N4R Tau (fused with a His_6-tag and the engineering TEV cleavage site). The bands after induction with 0.6, 0.8 and 1mM of IPTG displayed similar intensities and therefore 0.6 mM IPTG was chosen for the overexpressing in large scale (2 flasks of 1.5L each).

Table 5 - **Expression test for the WT 2N4R Tau fusion protein (with a N-terminal His_6-Tag and the engineering TEV cleavage site) in E. Coli BL21(DE3) cells.** OD_{600m} obtained before and after the induction with different IPTG concentrations.

Protein	IPTG concentrations (mM)	OD_{600nm}	
		Before IPTG induction	After IPTG induction
2N4R Tau fusion protein	0	0.853	1.690
	0.4	0.754	1.860
	0.6	0.800	1.896
	0.8	0.670	1.640
	1	0.600	1.738

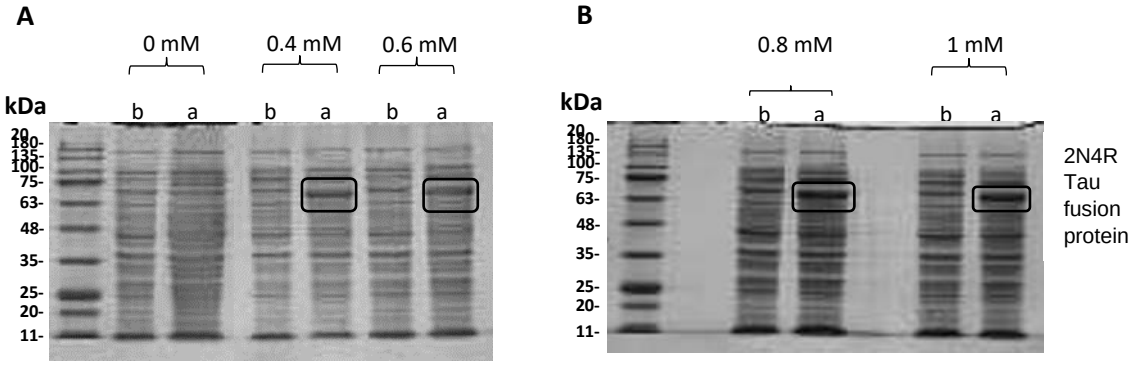

Figure 13 - SDS-PAGE analysis of the expression test samples for the WT 2N4R Tau fusion protein (with a N-terminal His_6-Tag and the engineering TEV cleavage site) before or after IPTG induction O/N at 16ºC.
A – IPTG concentrations: 0 mM, 0.4 mM and 0.6 mM. B - IPTG concentrations: 0.8 mM and 1 mM. b – Before IPTG induction and a – after IPTG induction. The black boxes highlight the bands corresponding to WT 2N4R Tau fusion protein. The marker NZYColour Protein Marker II was used in all gels.

3.1.2. Purification of WT 2N4R Tau – First Batch

As detailed above, the WT 2N4R Tau protein was expressed fused to a N-terminal His_6-tag and a TEV-cleavage site (DYDIPTT**ENLYFQ|G**S). Therefore, our purification strategy followed: (1) an initial IMAC to purify the Tau fusion protein from the cell lysate; (2) the cleavage of the His_6-tag by TEV protease (sequence ENLYFQ|G); (3) a second IMAC to purify WT 2N4R Tau from the His_6-tag, the fusion protein (not cleaved) and the TEV protease (containing also a His_6-tag), collecting the WT 2N4R Tau protein in the flow-through; and finally (4) a SEC for final purification of the WT 2N4R Tau protein.

The SDS-PAGE gels obtained during the WT 2N4R Tau purification (first batch) are shown in Figures 14. Tau is an intrinsically disordered protein (IDP) [44] and therefore it displays elongated shapes and higher hydrodynamic radius that lead to an atypical electrophoretic migration [45]. In particular, 2N4R Tau protein has a molecular weight (MW) of 45.85 kDa and the fusion protein has a MW of 48.55 kDa. Here Tau protein migrated in the SDS-PAGE gels between 63-75 kDa [45].

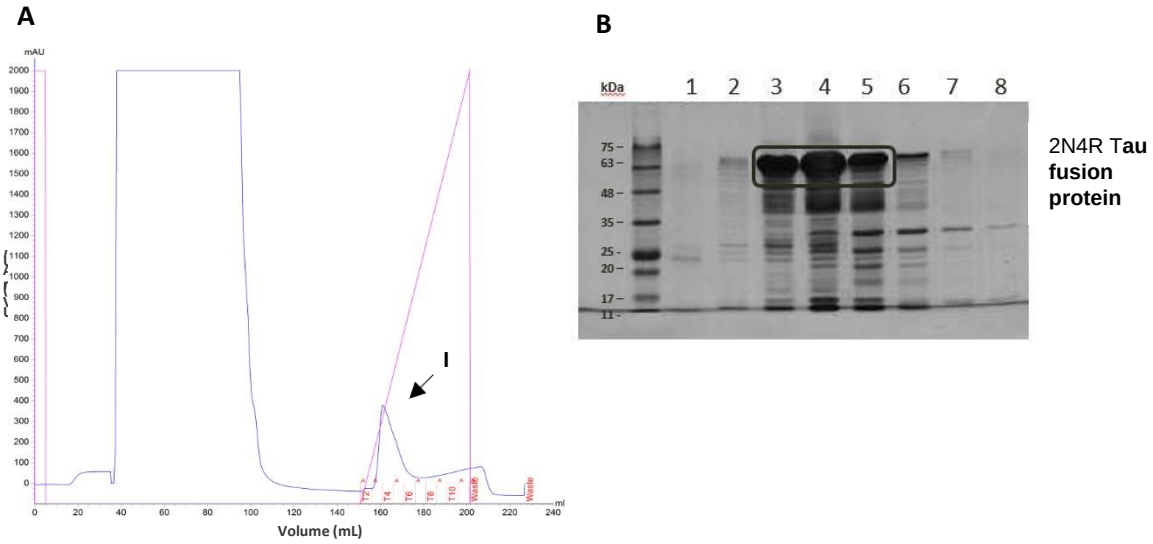

Figure 14 – First IMAC for the purification of WT 2N4R Tau (first purification step).

A – Chromatogram of the first IMAC (using a 5mL HisTrap™ FF column). Blue Line – UV at 280 nm; Pink Line – gradient with Nickel Buffer B; I – Elution peak (elution of Tau fusion protein). B –SDS-PAGE analysis of the fractions collected during the gradient with Nickel Buffer B; 1 – 8 represent the eluted fractions. The black box highlights the bands corresponding to the WT 2N4R Tau fusion protein. NZYColour Protein Marker II was used as protein standards.

The WT 2N4R Tau fusion protein was initially purified by IMAC from the cell lysate. In this IMAC, as Tau has a His_6-Tag, it initially bound to the HisTrap column (with nickel) and was then eluted during the gradient with Nickel buffer B (with higher Imidazole concentrations, in peak I of the chromatogram in figure 14). Fractions 3-5 of this peak were analysed by SDS-PAGE (figure 14). The Tau fusion protein corresponds to the band running between 63-75 kDa. This SDS-PAGE analysis also revealed that the Tau fusion protein was not completely pure.

Fractions 3 to 5 were then joined in an Amicon, exchange to Nickel Buffer A and finally concentrated to ~ 10 mL. We note that here we decreased the Imidozole concentration (for improving TEV cleavage). Then DTT and the TEV protease that recognizes the TEV-cleavage site (DYDIPTT**ENLYFQ|G**S, to remove the His_6-tag) were added and incubated O/N at 4ºC.

Afterwards, the buffer was changed to Nickel buffer A to remove the DTT and the second IMAC was performed. During this purification step, the WT 2N4R Tau protein was purified from the His_6-tag, the fusion protein (uncleaved protein) and the protease (TEV also contains a His_6-tag). The WT 2N4R Tau protein (without tag) was eluted in the flow-through that comprises the peak I of the chromatogram displayed in Figure 15. In addition, SDS-PAGE analysis of this flow-through, Fractions 3 to 12 showed an intense band running at ~63 kDa that corresponds to the WT 2N4R Tau protein.

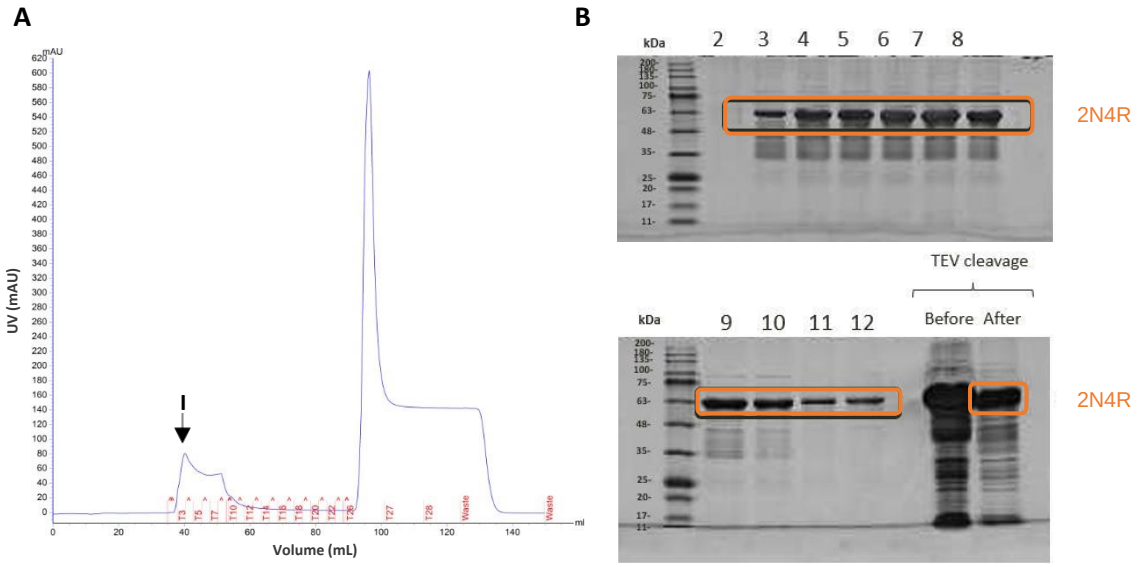

Figure 15 - Second IMAC for the purification of WT 2N4R Tau (second purification step).
A – Chromatogram of the second IMAC (using a 5mL HisTrap™ FF column). Blue Line – UV at 280 nm; I – Elution peak (elution of Tau protein). B –SDS-PAGE analysis of the fractions collected during the flow-through; 2 – 12 represent the eluted fractions; Before and after – before and after TEV cleavage samples. The orange box highlights the bands corresponding to the WT 2N4R Tau protein. NZYColour Protein Marker II was used as protein marker.

As some impurities remained after the second IMAC, we decided to perform a final SEC purification. Fractions 3-12 (containing WT 2N4R Tau) from the second IMAC were joined in an Amicon, buffer exchange to buffer C and concentrated to ~2 mL. The elution of WT 2N4R Tau protein in SEC started at ~60 mL (figure 16 A, peak I and Fractions 10-12). SDS-PAGE analysis also confirmed that Fractions 10-12 contained highly pure WT 2N4R Tau protein, with a band running at ~63kDa.

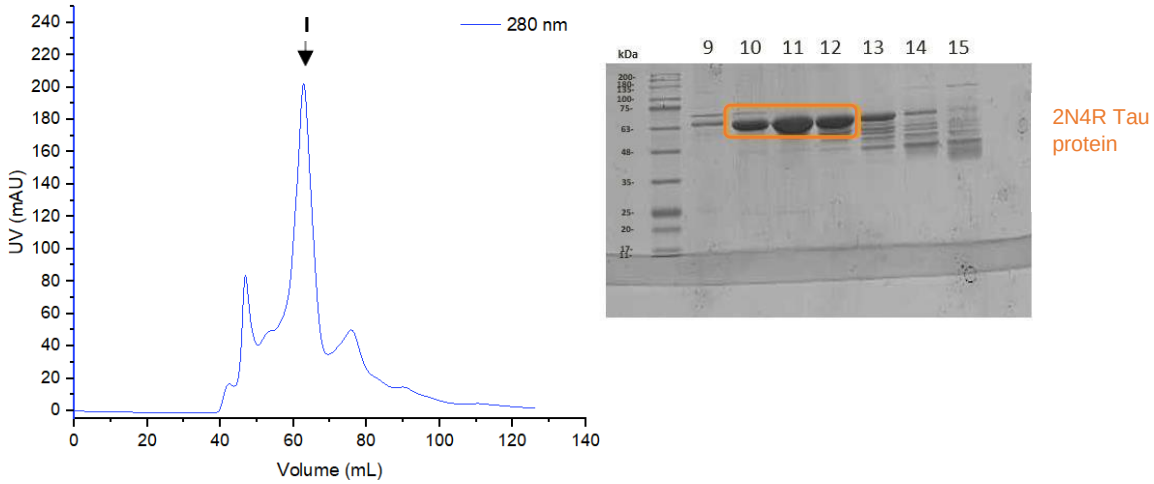

Figure 16 – SEC for the purification of WT 2N4R Tau (final purification step).
A – Chromatogram of the SEC (using a HiLoad 16/600 Superdex 200 column). *Blue Line* – UV at 280 nm; *I* – Elution peak (elution of WT 2N4R Tau protein). *B* –SDS-PAGE analysis of the fractions 9-15 collected during SEC; 10 – 12 - Fractions with pure Tau protein. The orange box highlights the bands corresponding to the WT 2N4R Tau protein. NZYColour Protein Marker II was used as protein marker.

The total protein concentration in Fractions 10, 11 and 12 was determined by UV_{280} nm (Nanodrop) using the molecular extinction coefficient of Tau (7450 M^{-1} cm^{-1}) [42], and the Pierce BCA Protein Assay Kit was employed for Fraction 11 (Table 6). Finally, the fractions were aliquoted in 150 µL and stored at -80ºC.

Table 6 - **Protein Concentration obtained for Fractions 10, 11 and 12. a –** Measurement of concentration using absorbance at 280 nm in a NanoDrop™ One/One (Thermo Fisher)**. b -** Measurement of concentration using the Pierce BCA Protein Assay Kit (from Thermo Fisher Scientific).

Fraction	Protein Concentration (µM)
10 [a]	18.6
11 [a]	22.8
11[b]	18.9
12 [a]	20.4

3.1.3. Expression and purification of WT 2N4R Tau – Second Batch

The ThT fluorescence assays employed in this thesis for monitoring Tau aggregation (in amyloid fibrils) require high protein concentrations, and therefore we repeated the production of WT 2N4R Tau protein.

We applied here the same purification strategy as described for the first batch (section 3.1.2). The chromatograms obtained for the second purification batch were identical to the first batch. The SDS-PAGE gels were also similar to the first batch Ffigure 17, A, B, C and D). After SEC, we obtained again highly pure WT 2N4R Tau protein in Fractions 12-14 (Figure 17, D). The protein concentration was again quantified by Abs_{280} nm and by Pierce BCA Protein Assay Kit (Table 7).

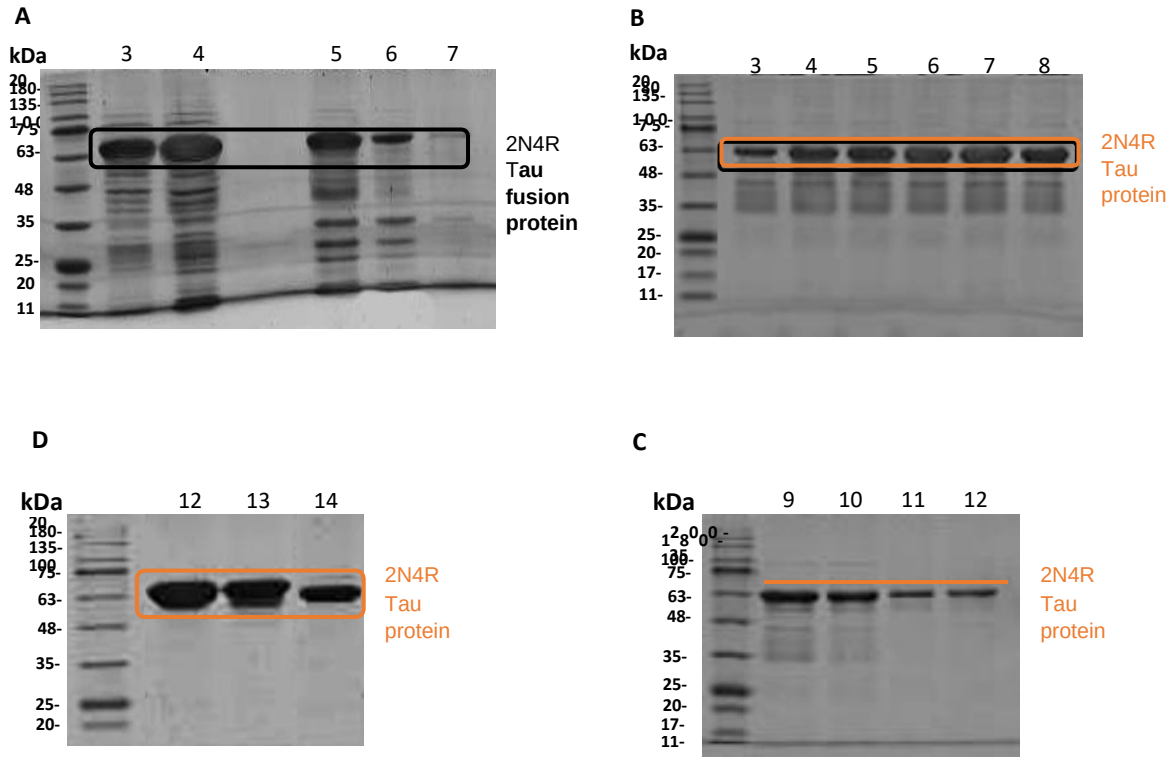

Figure 17 - SDS-PAGE analysis of WT 2N4R Tau purification of the second batch.

A – First IMAC. The WT 2N4R Tau fusion protein (highlighted in black box) was eluted in Fractions 3-6, during the gradient with Nickel Buffer B. **B and C** – Second IMAC. Fractions 3-12 containing the WT 2N4R Tau (without tag, black box) were collected in the flow-through. **D** – A SEC was performed for the final purification, and the WT 2N4R Tau protein was eluted in Fractions 12-14. The black box highlights the bands corresponding to the pure WT 2N4R Tau protein. In all SDS-Page gels, the marker NZYColour Protein Marker II was used.

Table 7 - Protein Concentration of the fractions containing pure WT 2N4R Tau protein from the second batch (12, 13 and 14). a - Measurements by Abs280 nm (Nanodrop). b - Measurement by Pierce BCA Protein Assay Kit.

Fraction	Protein Concentration (μM)
12[a]	29.5
13[a]	26.8
13[b]	20.8
14[a]	20.0

3.2. Expression and Purification of P301L 2N4R Tau

3.2.1. Site-Directed Mutagenesis

The P301L mutation in Tau protein is one of the most studied disease point-mutations associated with Tauopathies, including frontotemporal dementia with parkinsonism linked to chromosome 17 (FTDP-17) [8]. P301L mutation impacts Tau binding/stabilization of microtubules and increases its aggregation [15].

The original pET-HT-Tau plasmid encodes for the WT 2N4R Tau protein, and therefore we engineered it for the expression of P301L 2N4R Tau by site-directed mutagenesis. We employed the QuikChange II Site-Directed Mutagenesis method (from Agilent) and the plasmids were purified/extracted by the NZYMiniprep (form) for subsequent sequencing. There were some initial problems with the introduction of the P301L mutation and only the original sequence was obtained. Therefore, a new DpnI enzyme was used and afterwards the P301L mutation was successfully introduced. Figure 17 shows the alignment of the genes for WT (original) and P301L variants. We note that 2 primers (T7 Terminator and T7 forward) were used for covering all gene (more than 1100 bases) and to guarantee that no further mutations were introduced or sequence deleted.

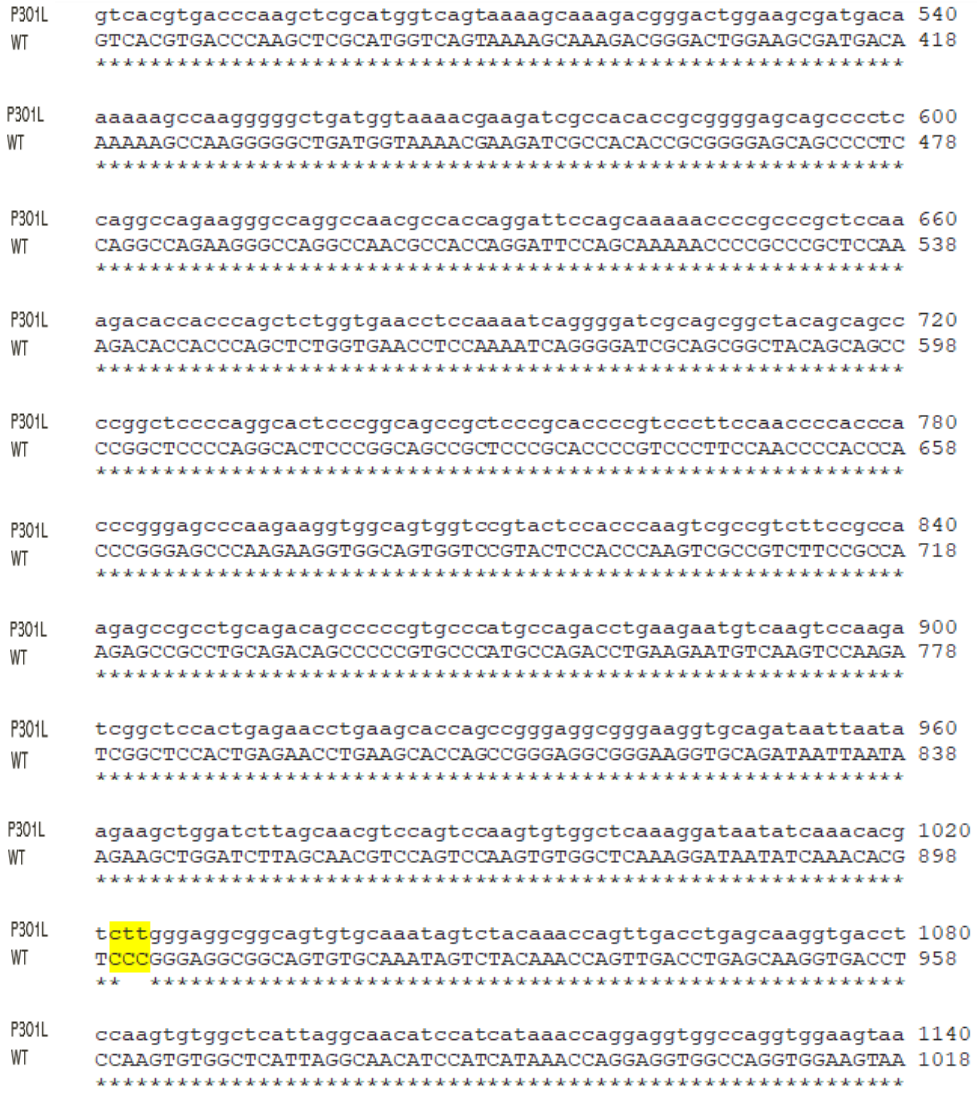

Figure 18 – Sequence alignment of the P301L 2N4R Tau gene against the WT variant. The alignment was performed with T7 Terminator and T7 Forward primes using the Clustal Omega. At yellow is highlighted the codon mutated for the P301L mutation.

3.2.2. Expression and Purification of P301L 2N4R Tau

The P301L 2N4R Tau protein was purified as described before for the WT variant. The chromatograms and SDS-PAGE gels (Figure 19) obtained here were also identical to the ones obtained for the WT 2N4R Tau protein (for both batches).

We obtained highly pure P301L 2N4R Tau protein after SEC (Fractions 10-12) (Figure 19, C) that was then stored in 150 µL aliquots at -80ºC. The protein concentration was also measured by Abs280 nm and using the Pierce BCA Protein Assay Kit (Table 8). The concentrations obtained for P301L 2N4R Tau protein were lower than those obtained for WT protein.

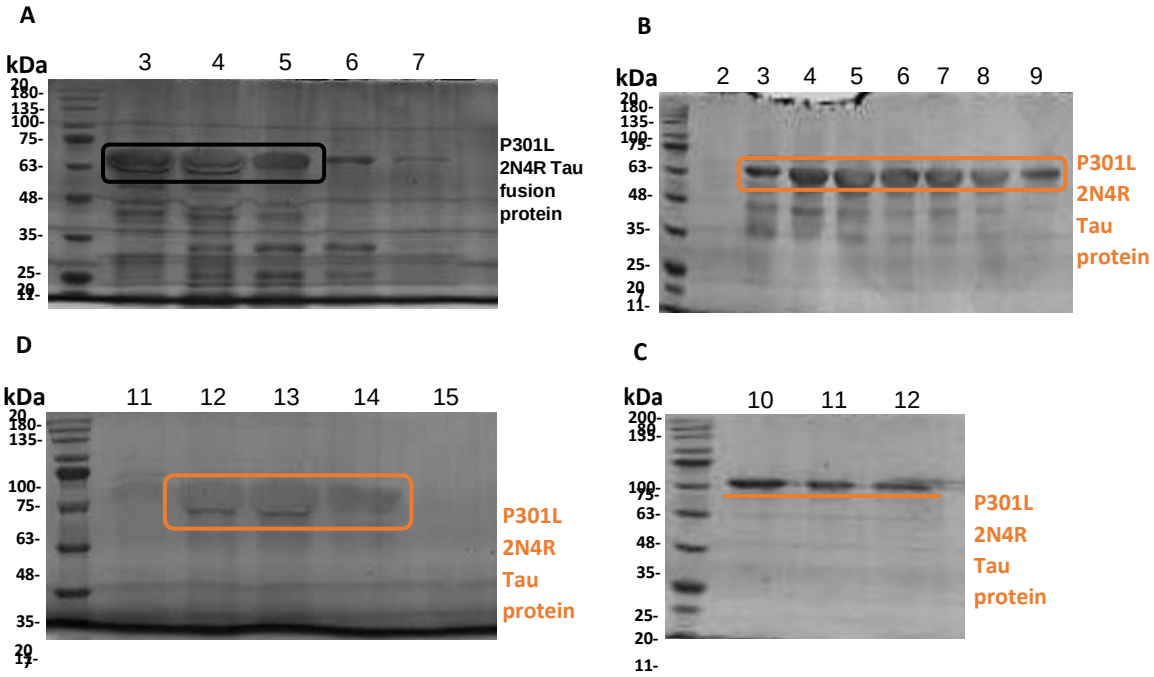

Figure 19 - SDS-PAGE analysis of P301L 2N4R Tau purification. A – First IMAC. The P301L 2N4R Tau fusion protein was eluted in Fractions 3-7 during the gradient with Nickel Buffer B. **B and C** – Second IMAC. Fractions 3-14 containing the P301L 2N4R Tau were collected in the flow-through. **D** – A SEC was again performed for the final purification of P301L 2N4R Tau protein (Fractions 12-14). The black box highlights the bands corresponding to the P301L 2N4R Tau fusion protein and the orange boxs indicate the bands corresponding to the pure P301L 2N4R Tau protein (without tags). In all SDS-Page gels, the marker NZYColour Protein Marker II was used.

Table 8 - Protein concentration of the fractions 12 and 13 (after SEC) containing pure P301L 2N4R Tau protein. a - Measurements by Abs280 nm (Nanodrop). b - Measurement by Pierce BCA Protein Assay Kit.

Fraction	Protein Concentration (μM)
12[a]	16.1
12[b]	19.9
13[a]	16.2

3.3. Expression and Purification of TEV protease

TEV protease was expressed in *E. coli* BL21(DE3) cells using 1mM IPTG and at 37ºC for 4 hours. For SDS-PAGE analysis, samples were collected before and after IPTG induction (Figure 20), showing that TEV was successfully expressed after adding IPTG and run at ~25 kDa in the gel.

As TEV was expressed with a His_7-tag, its purification was carried out by an IMAC. The His_7-TEV protein initially bound to the column and was subsequently eluted during the gradient of buffer B_{TEV}. As shown in the SDS-PAGE gels in figure 20, the TEV after IMAC purification already appeared highly pure (band running at ~25 kDa) and therefore it did not require further purification by SEC. Finally, a dialysis was performed (for Fractions 2-9) for exchanging to buffer $TEV_{storage}$ (with glycerol). The concentration was quantified by measuring the Abs280nm. The concentration was then calculated with the molecular extinction coefficient of Tau: 7450 M−1 cm−1 [42], and the concentration was 34.9 µM.

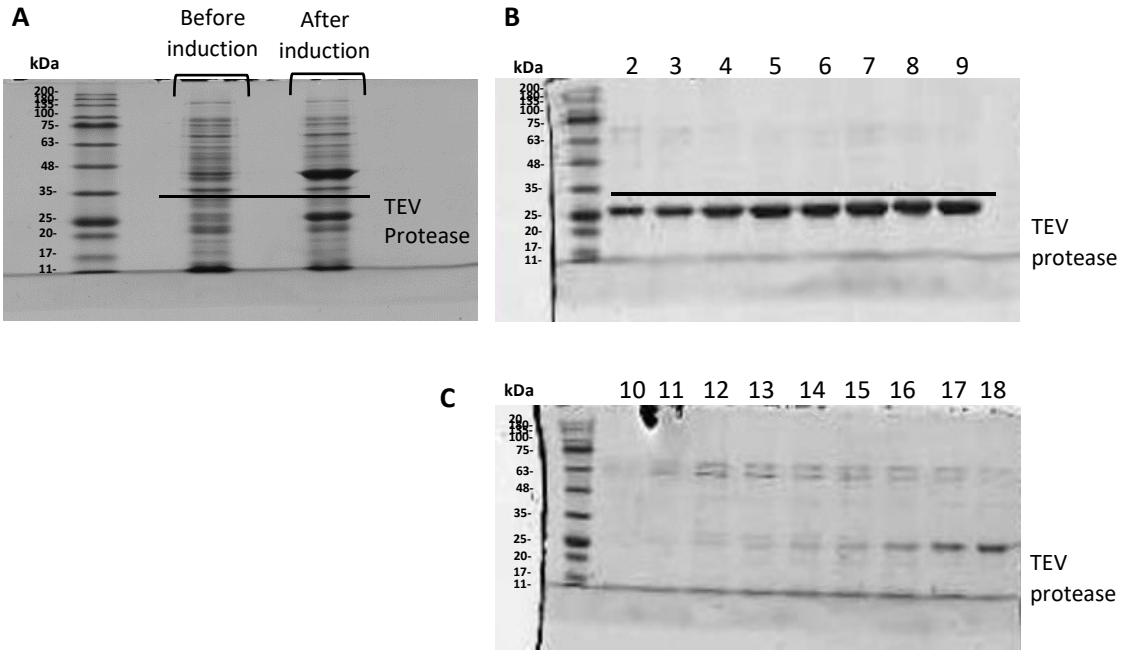

Figure 20 - SDS-PAGE analysis of the expression and purification of TEV protease. A – Samples before and after induction with IPTG. B and C –SDS-PAGE analysis of the IMAC fractions (2-18) collected during the gradient with buffer B_{TEV}; The black boxes highlight the bands corresponding to TEV protease. The marker NZYColour Protein Marker II was used in all gels.

3.4. ThT fluorescence assays

ThT fluorescence assays have been widely employed for monitoring Tau fibrillation *in vitro*. However, most of the aggregation biophysical studies have been performed so far with the K18 Tau fragment that only comprises the MTBR domain [46]. In the scope of this thesis, we evaluated the aggregation of 2N4R Tau (longest isoform) of both WT and P301L variants in the presence of two anionic aggregation-inducers, including heparin and POPS-containing lipid vesicles. The concentrations of Tau protein and aggregation inducers used during these experiments are shown in Table 9. We note that we carried out more assays (here not presented)

that unfortunately were interrupted due to issues in the microplate reader itself or electricity cuts in the equipment room.

Table 9 - Summary of the ThT fluorescence assays performed for monitoring the 2N4R Tau fibrillation (for WT and P301L variants).

Assay Number	Protein used and Batch Number	[Protein] (μM)	[Heparin] (mg/mL)	[LUVs] (μM)
Assay 1	WT 2N4R Tau (Batch 1)	10	-	-
Assay 2	WT 2N4R Tau (Batch 1)	22.8	-	-
Assay 3	WT 2N4R Tau (Batch 1)	22.8	0.5 and 1.0	-
Assay 4	WT 2N4R Tau (Batch 2)	20	0.5 and 1.0	-
Assay 5	WT 2N4R Tau (Batch 2)	20	0.5 and 1.0	-
Assay 6	P301L 2N4R Tau	20	0.5	50 and 100
Assay 7	WT 2N4R Tau (Batch 2) and P301L 2N4R Tau	20	0.5	25 and 50

3.4.1. Tau fibrillation in solution and controls

We initially performed the ThT fluorescence assays with WT 2N4R Tau protein in solution with distinct concentrations - 10 and 22.8 μM (from batch 1) (Figure 21). Specifically, this WT variant was incubated with 50 μM ThT in 50 mM Tris pH 7.4, 1 mM DTT, and 50 mM NaCl buffer, for 7-days at 37 ºC (with orbital shaking before each measurement). For 10 μM of WT 2N4R Tau protein, we did not detect any significant change in the ThT signal during the assay, reporting that protein fibrillation did not occur. When the protein concentration was increased to 22.8 μM (also from batch 1), the ThT fluorescence intensity increased upon 2-days and reached ~2100 a.u. at the 7th-day, but the magnitude of changes in the ThT signal was still lower (from 1000 to 2100 a.u.). For the second batch of WT 2N4R Tau protein, we conducted all assays with 20 μM of protein. Here, we detected some variability within the assays, but the increase in ThT fluorescence intensity was minor or not occurred, showing that the WT 2N4R Tau protein was not aggregating extensively in solution during our measurements.

In parallel, we also performed ThT fluorescence assays with 20 μM of P301L 2N4R Tau protein in solution (Figure 21). As for the WT protein, the ThT signal remained almost invariant during the assay for this mutant protein, revealing that the P301L mutation did not enforce extensive aggregation of Tau protein in solution.

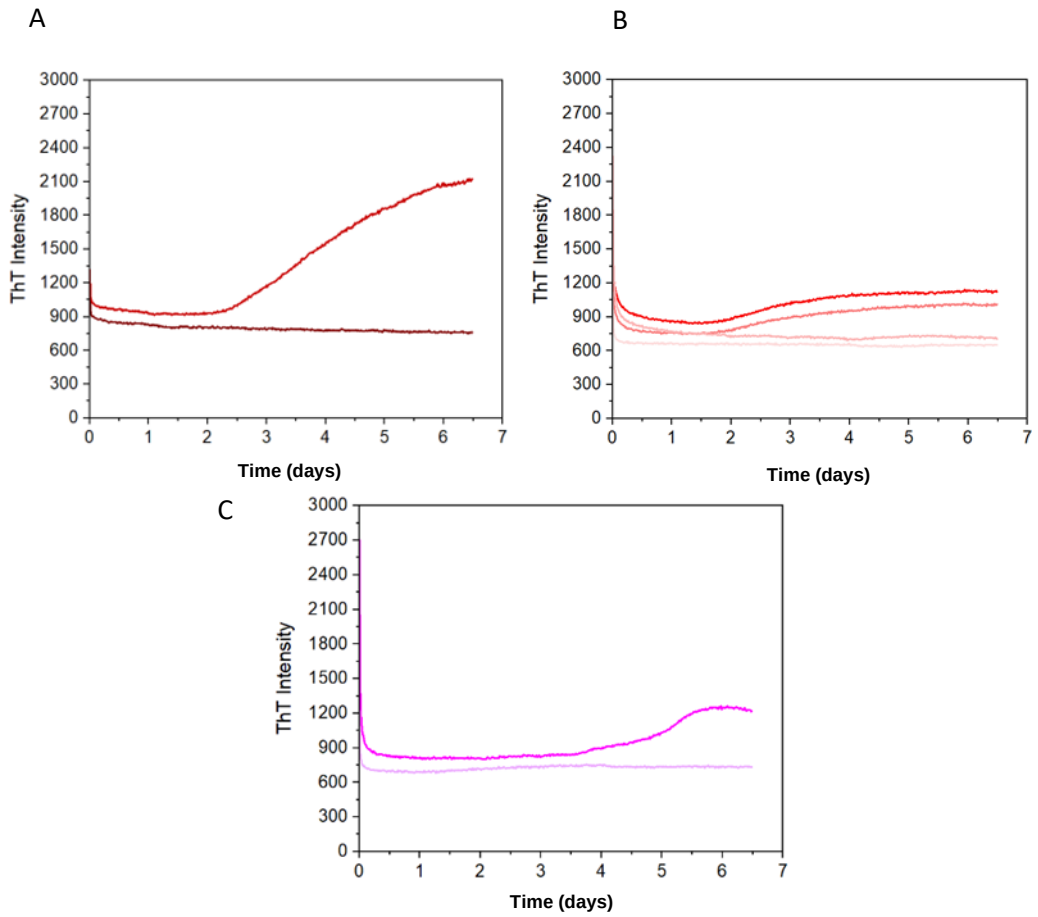

Figure 21 - ThT fluorescence assays for WT and P301L 2N4R Tau protein in solution (50 mM Tris pH 7.4, 1 mM DTT, and 50 mM NaCl buffer). ThT fluorescence intensities upon incubation with: (A) 10 and 22.8 μM (assay 1 (dark red) and 2 (light red) and (B) 20 μM of WT 2N4R Tau (assays 3 to 5 (from darkestto lightest red, respectively) and 7 (lighter shade of red))**;** and with (C) 20 μM of P301L 2N4R Tau (assays6 (darkest purple) and 7 (lightest purple)). Red – WT 2N4R Tau in solution; Purple – P301L 2N4R Tau in solution.

In figure 22 is shown the different controls carried out during our assays. For all the controls, ThT fluorescence intensities remained very low and constant over the experiment (for 7-days), in buffer and in the presence of both heparin and liposomes. These data show that ThT does not bind to both aggregation inducers.

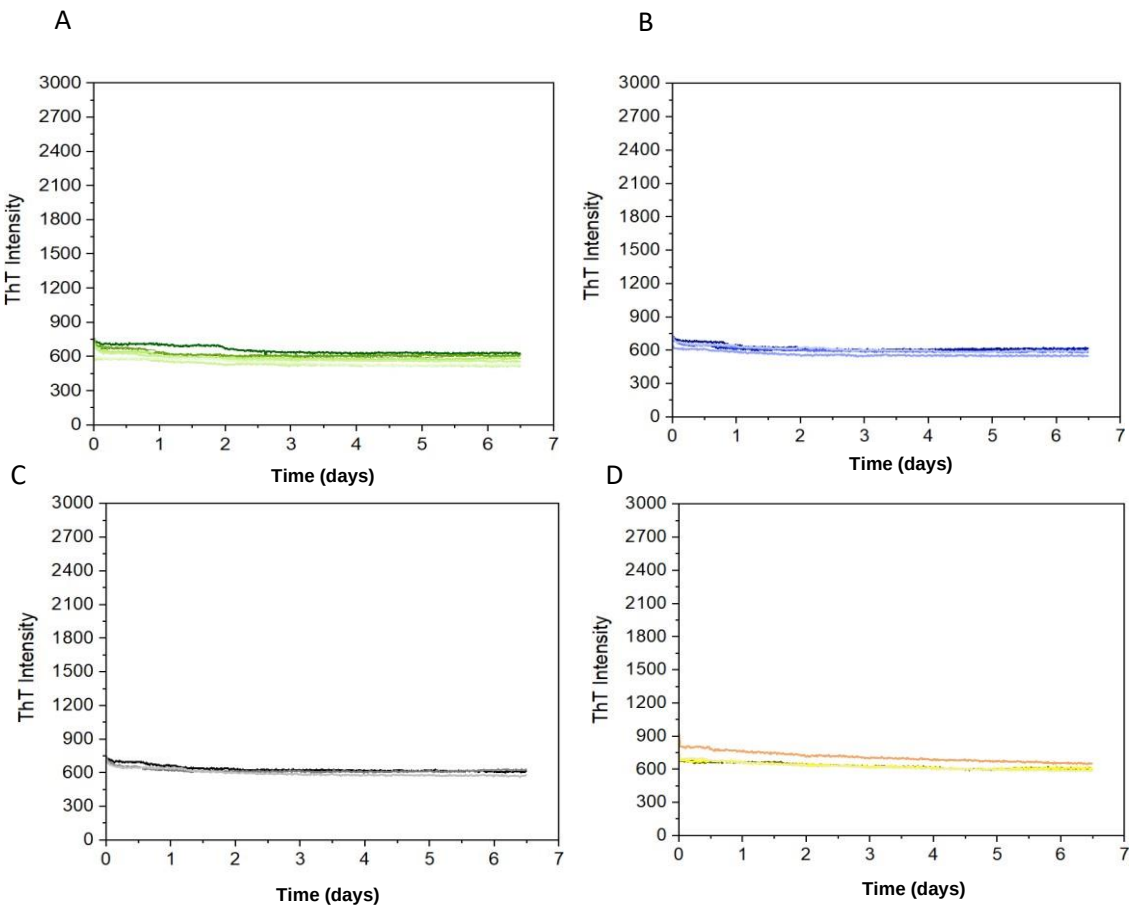

Figure 22 - ThT fluorescence intensities for control samples. A in buffer (green), B in the presence of 0.5 mg/mL heparin (blue), C – in the presence of 1.0 mg/mL heparin (gray), and finally D – upon incubation with LUVs (yellow).

3.4.2. Tau fibrillation in the presence of heparin

As previously mentioned, Tau aggregation can be triggered by anionic inducers, such as polyanions like heparin. In particular, heparin compensates for the repulsive positive charges of Tau and stabilizes an aggregation-prone conformation [23]. Moreover, adding heparin will result in the formation of filamentous structures [47].

For the WT 2N4R Tau protein, ThT fluorescence assays were performed with 22.8 µM or 20 µM of Tau protein incubated with 0.5 mg/mL and 1 mg/mL of heparin (Figure 23). We note that these assays with heparin lack reproducibility, particularly in the absolute values of ThT fluorescence intensities. Therefore, the heparin data were not averaged and only a qualitative analysis was performed. However, for all assays, the ThT signal increased significantly in the presence of heparin compared to solution conditions (only protein).

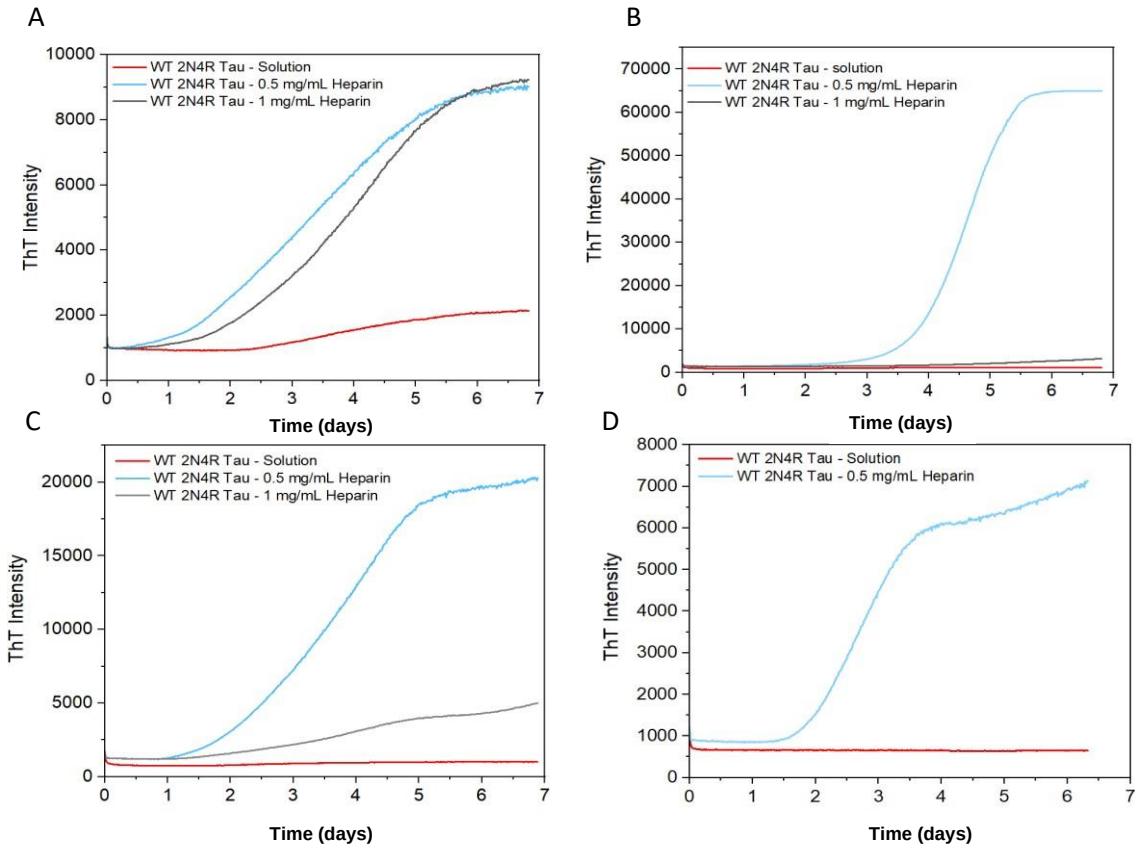

Figure 23 - ThT fluorescence assays for WT 2N4R Tau with heparin. ThT fluorescence intensity upon incubation WT 2N4R Tau in solution (red) and in the presence of 0.5 (blue) and 1 (gray) mg/ml of heparin. A- A*ssay* 3. B – Assay 4. C – Assay 5. D – assay 7.

In assay 3 (Figure 23 A) with 22.8 µM of WT protein (batch 1), the ThT signal in the presence of both heparin concentrations shows a typical sigmoid profile (with similar variations) and reached nearly the same plateau (~9200 and ~9300 a.u.). In assay 4 (Figure 23) with 20 µM of WT Tau protein (batch 2), the ThT fluorescence only increased in the presence of 0.5 mg/ml of heparin and its signal was saturated. For assays 5 and 7 (Figure 23 C and D) with 20 µM of WT protein (batch 2), the profile of variations in the ThT signal was similar with 0.5 mg/ml of heparin (although distinct in absolute values, reaching a plateau of ~20 000 and ~7000, respectively) and their intensities started to increase before the second day.

The ThT fluorescence assays with 20 µM of P301L 2N4R Tau were performed only with 0.5 mg/mL of heparin (Figure 24). Here, we employed the same conditions as detailed for WT 2N4R Tau (for 7 days at 37°C with orbital shaking before each measurement). Although the magnitude of changes in the ThT signal was different for both assays (reaching a plateau at ~30,000 and ~60,000), our data show that the kinetics of P301L 2N4R fibrillation in the presence of 0.5 mg/ml heparin were faster than WT protein as ThT signal increased after a few hours.

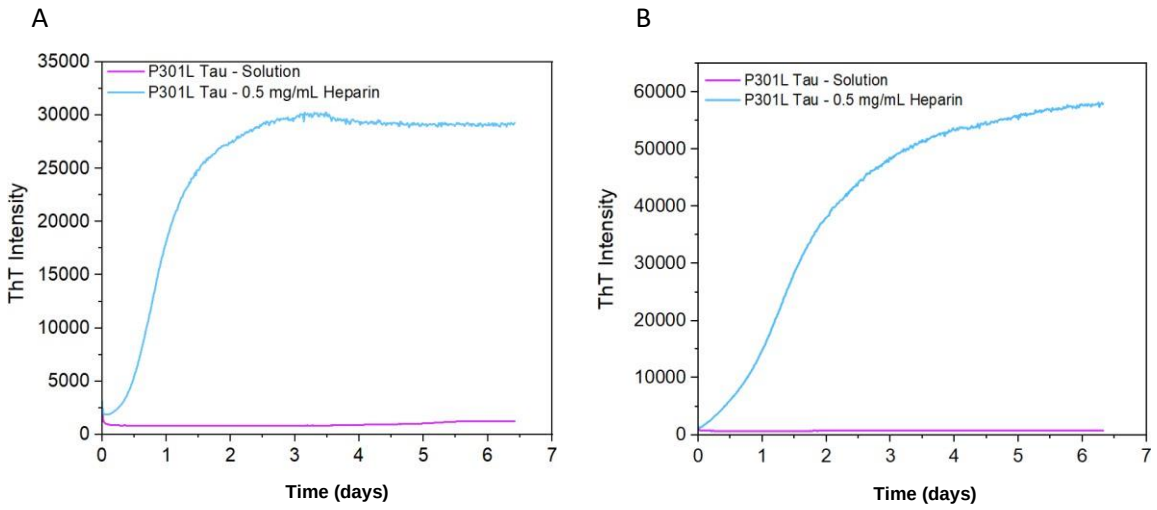

Figure 24 - ThT fluorescence assays for P301L 2N4R Tau with heparin. ThT fluorescence intensity upon incubation P301L 2N4R Tau in solution (purple) and in the presence of 0.5 mg/mL of heparin (blue). A – Assay 6. B – Assay 7.

3.4.3. Tau fibrillation in the presence of anionic lipid vesicles

We next sought to investigate the role of anionic lipid vesicles in Tau aggregation. ThT fluorescence assays were performed for 2N4R Tau protein (both P301L and WT) in the presence of 50:50 POPC:POPS LUVs (Figure 25). Since anionic lipid vesicles induce Tau aggregation, it was one of the inducers used for the study [48].

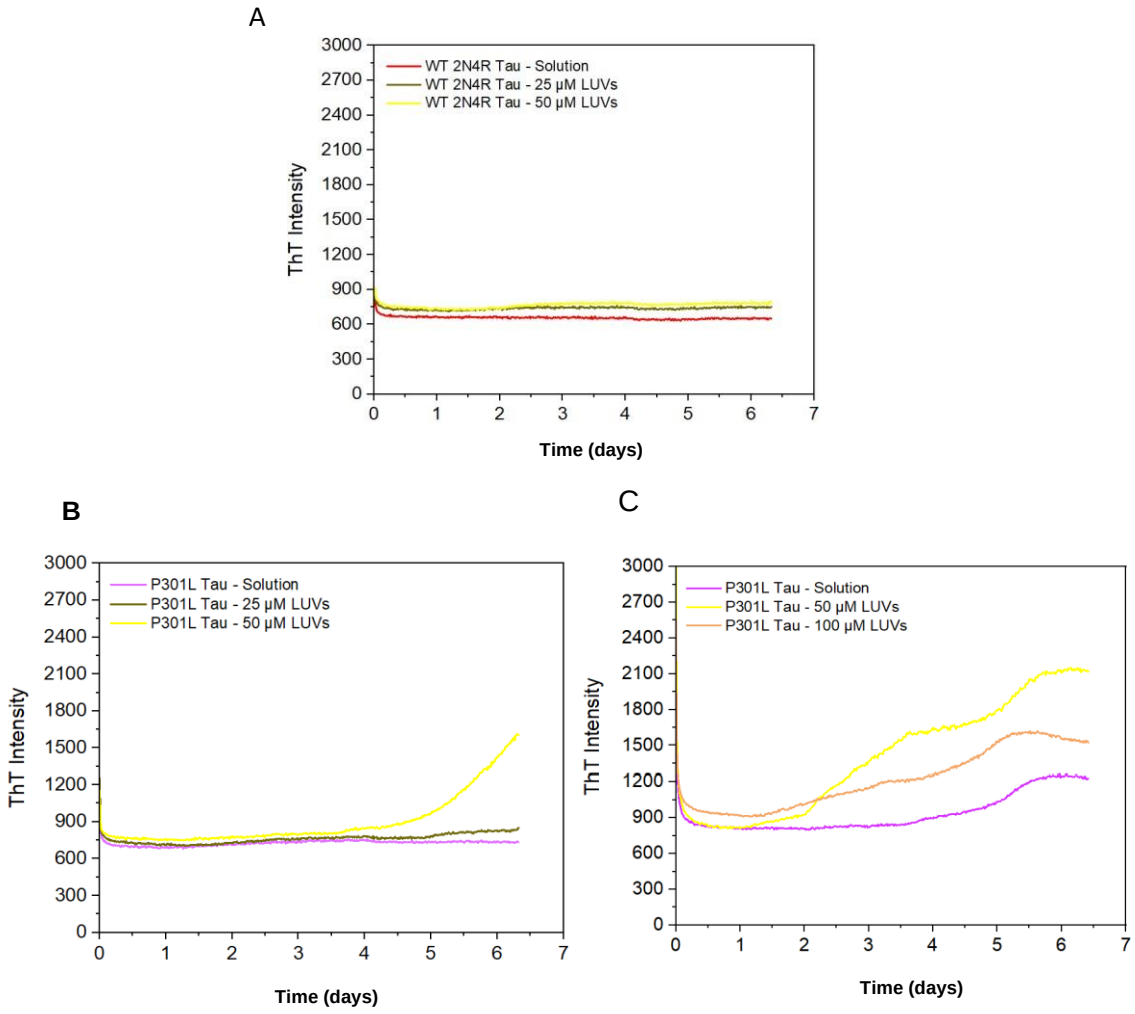

Figure 25 - ThT fluorescence assays for WT and P301L 2N4R Tau with LUVs. A – assay 7. B – assay 7. C – assay 6. Brown – P301L 2N4R Tau with 25 µM of LUVs. Yellow - P301L 2N4R Tau with 50 µM of LUVs. Orange - P301L 2N4R Tau with 100 µM of LUVs. Purple – P301L 2N4R Tau in solution. In all figures, WT and P301L 2N4R Tau was used as a control.

For WT 2N4R Tau, the ThT signal remained invariant in the presence of 50:50 POPC:POPS LUVs (25 and 50 µM), revealing that anionic membranes were not able to trigger Tau fibrillation in our experiments, but is not possible to take many conclusions, since only two assays were carried out, it would be necessary to carry out more assays. For P301L 2N4R Tau protein, the fluctuations in ThT signal was not significant upon incubation with LUVs, considering the magnitude of changes for buffer and a 7-days assay.

To also monitor Tau aggregation/fibrillation, a SDS-PAGE analysis was performed for Assay 7, taking samples at the beginning and at end of the ThT fluorescence assay (Figure 26). Globally, the data show that some fraction of 2N4R Tau protein was not incorporated in fibrils, as it was still observed a typical band for this protein for samples taken at the end of the assay. For a complete fibrillation, this band should have disappeared as fibrils are not able to run in the SDS-PAGE gel or will appear at the top.

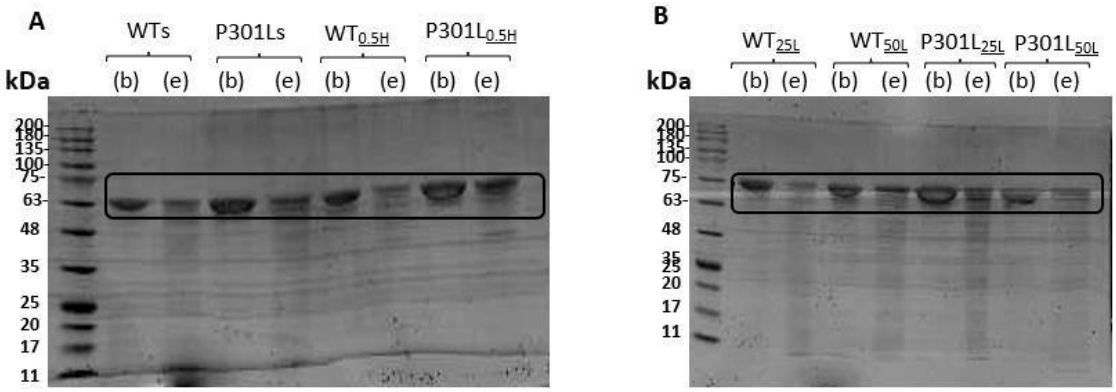

Figure 26 - SDS-PAGE analysis of the samples collected at the beginning and at the end of assay 7. Samples were taken at the beginning (b) and end of the assay (e) for protein (B) in solutions and with heparin and (B) with LUVs. The typical band of WT 2N4R Tau and P301L Tau is identified with a black box. WTs- WT 2N4R Tau in solution; P301Ls -P301L Tau in solution; $WT_{0.5H}$ - WT 2N4R Tau with 0.5 mg/mL heparin; $P301L_{0.5H}$ - P301L Tau with 0.5 mg/mL heparin. WT_{25L} - WT 2N4R Tau with 25 µM LUVs; WT_{50L} WT 2N4R Tau with 50 µM LUVs; $P301L_{25L}$ - P301L Tau with 25 µM LUVs; $P301L_{50L}$ -P301L Tau with 50 µM LUVs.

4. Conclusion

The pathological self-assembly of Tau protein into neurofibrillary tangles in neurons is associated with several devastating Tauopathies. These include AD, Parkinson's disease, Lewy body dementia, Pick's disease [13]. In particular, the hyperphosphorylation of Tau and disease mutations (such as P301L at R2 in MTBR) lead to a disruption of Tau's ability to bind and stabilize microtubules and also increase its tendency to form filaments [15].

Tau aggregation *in vitro* has been extensively studied by performing ThT fluorescence assays to monitor the formation of amyloid fibrils. These studies have been performed so far with the K18 Tau fragment, which only comprises the MTBR [46]. This fragment contains the core of the aggregates found in disease, but lacks the N-projection domain, proline-rich region and C-terminal [46]. Moreover, there are only a few studies focused on the aggregation of WT and P301L 2N4R Tau isoform with heparin, and in the presence of lipids has been largely overlooked [49, 50, 51]. In addition, these ThT assays are not standardized across different labs regarding the experimental conditions employed (such as the buffer, continuous or not shaking, etc), making challenging their systematic analysis.

Therefore, during this thesis, we recombinantly expressed/purified WT and P301L 2N4R Tau proteins, and in parallel we also performed ThT fluorescence assays of both WT and P301L variants in solution and in incubation with anionic aggregation-inducers, such heparin and POPS-containing liposomes.

Our ThT fluorescence assays show some variability within the absolute values of fluorescence intensities [49, 52]. But overall, the data indicate that heparin strongly promote Tau fibrillation, as the fibrillation kinetics were faster in the presence of heparin. In particular, both WT and P301L were not undergoing extensive aggregation in solution (the magnitude of changes in the ThT signal was lower over 7-days assay). Our studies also revealed that heparin imposes a faster aggregation kinetics for P301L mutant, as the increase in ThT signal started in a few hours.

We also conducted ThT fluorescence assays of both 2N4R Tau proteins (WT and P301L) with anionic lipid membranes (50:50 POPC:POPS LUVs). For WT 2N4R Tau, we didn´t detect any change in the ThT signal and for P301L variant, the fluctuations on the ThT signal were not significative (comparing with heparin conditions with a high magnitude of variations). As anionic lipid membranes have been reported as an aggregation-inducers (using K18 fragment) [46], future experiments should explore liposomes with a higher anionic lipid content and also using even higher protein concentrations.

Taken together our results, heparin is a stronger aggregation-promoter of 2N4R Tau protein than anionic lipids, and in particular in a higher magnitude for P301L Tau. Finally, in the future, to follow the early steps of aggregation (as oligomers not detected by ThT), anisotropy measurements could be also performed.

5. References

[1] Rachakonda V, Pan TH, Le WD. Biomarkers of neurodegenerative disorders: How good are they? *Cell Res*. 2004;14(5):349-358. doi:10.1038/sj.cr.7290235

[2] Scheltens P, De Strooper B, Kivipelto M, et al. Alzheimer's disease. *Lancet*. 2021;397(10284):1577-1590. doi:10.1016/S0140-6736(20)32205-4

[3] Goedert M. Tau protein and neurodegeneration. *Semin Cell Dev Biol*. 2004;15(1):45-49. doi:10.1016/j.semcdb.2003.12.015

[4] Anwal L. a Comprehensive Review on Alzheimer'S Disease. *World J Pharm Pharm Sci*. 2021;10(7):1170. doi:10.20959/wjpps20217-19427

[5] 2020 Alzheimer's disease facts and figures. *Alzheimer's Dement*. 2020;16(3):391-460. doi:10.1002/alz.12068

[6] Masters CL, Bateman R, Blennow K, Rowe CC, Sperling RA, Cummings JL. Alzheimer's disease. *Nat Rev Dis Prim*. 2015;1:1-18. doi:10.1038/nrdp.2015.56

[7] Hernández F, Ferrer I, Pérez M, Zabala JC, del Rio JA, Avila J. Tau Aggregation. *Neuroscience*. Published online 2022:1-6. doi:10.1016/j.neuroscience.2022.04.024

[8] Brunello CA, Merezhko M, Uronen RL, Huttunen HJ. Mechanisms of secretion and spreading of pathological tau protein. *Cell Mol Life Sci*. 2020;77(9):1721-1744. doi:10.1007/s00018-019-03349-1

[9] Georgieva ER, Xiao S, Borbat PP, Freed JH, Eliezer D. Tau binds to lipid membrane surfaces via short amphipathic helices located in its microtubule-binding repeats. *Biophys J*. 2014;107(6):1441-1452. doi:10.1016/j.bpj.2014.07.046

[10] Chong FP, Ng KY, Koh RY, Chye SM. Tau Proteins and Tauopathies in Alzheimer's Disease. *Cell Mol Neurobiol*. 2018;38(5):965-980. doi:10.1007/s10571-017-0574-1

[11] Buée L, Bussière T, Buée-Scherrer V, Delacourte A, Hof PR. Tau protein isoforms, phosphorylation and role in neurodegenerative disorders. *Brain Res Rev*. 2000;33(1):95-130. doi:10.1016/S0165-0173(00)00019-9

[12] Šimić G, Babić Leko M, Wray S, et al. Tau protein hyperphosphorylation and aggregation in alzheimer's disease and other tauopathies, and possible neuroprotective strategies. *Biomolecules*. 2016;6(1):2-28. doi:10.3390/biom6010006

[13] Guo T, Noble W, Hanger DP. Roles of tau protein in health and disease. *Acta Neuropathol*. 2017;133(5):665-704. doi:10.1007/s00401-017-1707-9

[14] Goedert M, Spillantini MG. Propagation of Tau aggregates Tim Bliss. *Mol Brain*. 2017;10(1):1-9. doi:10.1186/s13041-017-0298-7

[15] Miyasaka T, Morishima-Kawashima M, Ravid R, Kamphorst W, Nagashima K, Ihara Y. Selective deposition of mutant tau in the FTDP-17 brain affected by the P301L mutation. *J Neuropathol Exp Neurol*. 2001;60(9):872-884. doi:10.1093/jnen/60.9.872

[16] Barghorn S, Zheng-Fischhofer Q, Ackmann M, et al. Structure, microtubule interactions, and paired helical filament aggregation by tau mutants of frontotemporal dementias. *Biochemistry*. 2000;39(38):11714-11721. doi:10.1021/bi000850r

[17] Strang KH, Golde TE, Giasson BI. MAPT mutations, tauopathy, and mechanisms of neurodegeneration. *Lab Investig*. 2019;99(7):912-928. doi:10.1038/s41374-019-0197-x

[18] Niewiadomska G, Niewiadomski W, Steczkowska M, Gasiorowska A. Niewiadomska, G., Niewiadomski, W., Steczkowska, M., & Gasiorowska, A. (2021). Tau Oligomers Neurotoxicity. Life (Basel, Switzerland), 11(1), 28. https://doi.org/10.3390/life11010028. 2021;(iv).

[19] Rodrigues F, Oh H. Proteína Tau E As Doenças Neurodegenerativas. *Rev Científica Cogn*. 2021;2215:3355-3364. doi:10.38087/2595.8801.90

[20] Von Bergen M, Friedhoff P, Biernat J, Heberle J, Mandelkow EM, Mandelkow E. Assembly of τ protein into Alzheimer paired helical filaments depends on a local sequence motif (306VQIVYK311) forming β structure. *Proc Natl Acad Sci U S A*. 2000;97(10):5129-5134. doi:10.1073/pnas.97.10.5129

[21] Khlistunova I, Biernat J, Wang Y, et al. Inducible expression of tau repeat domain in cell models of tauopathy: Aggregation is toxic to cells but can be reversed by inhibitor drugs. *J Biol Chem*. 2006;281(2):1205-1214. doi:10.1074/jbc.M507753200

[22] Kadavath H, Hofele R V., Biernat J, et al. Tau stabilizes microtubules by binding at the interface between tubulin heterodimers. *Proc Natl Acad Sci U S A*. 2015;112(24):7501-7506. doi:10.1073/pnas.1504081112

[23] Ramachandran G, Udgaonkar JB. Understanding the kinetic roles of the inducer heparin and of rod-like protofibrils during amyloid fibril formation by tau protein. *J Biol Chem*. 2011;286(45):38948-38959. doi:10.1074/jbc.M111.271874

[24] Braak E, Braak H, Mandelkow E-M. A sequence of cytoskeleton changes related to the formation of neurofibrillary tangles and neuropil threads. *Acta Neuropathol*. 1994;87(6):554-567. doi:10.1007/s004010050124

[25] Cohen SIA, Vendruscolo M, Dobson CM, Knowles TPJ. From macroscopic measurements to microscopic mechanisms of protein aggregation. *J Mol Biol*. 2012;421(2-3):160-171. doi:10.1016/j.jmb.2012.02.031

[26] Lee S, Liu Y, Lim MH. Untangling Amyloid- β , Tau, and Metals in Alzheimer ' s Disease. Published online 2013.

[27] Munishkina LA, Fink AL. Fluorescence as a method to reveal structures and membrane-interactions of amyloidogenic proteins. *Biochim Biophys Acta - Biomembr*. 2007;1768(8):1862-1885. doi:10.1016/j.bbamem.2007.03.015

[28] Biancalana M, Koide S. Molecular mechanism of Thioflavin-T binding to amyloid fibrils. *Biochim Biophys Acta - Proteins Proteomics*. 2010;1804(7):1405-1412. doi:10.1016/j.bbapap.2010.04.001

[29] Khurana R, Coleman C, Ionescu-Zanetti C, et al. Mechanism of thioflavin T binding to amyloid fibrils. *J Struct Biol*. 2005;151(3):229-238. doi:10.1016/j.jsb.2005.06.006

[30] Krebs MRH, Bromley EHC, Donald AM. The binding of thioflavin-T to amyloid fibrils: Localisation and implications. *J Struct Biol*. 2005;149(1):30-37. doi:10.1016/j.jsb.2004.08.002

[31] Sulatskaya AI, Maskevich AA, Kuznetsova IM, Uversky VN, Turoverov KK. Fluorescence quantum yield of thioflavin T in rigid isotropic solution and incorporated into the amyloid fibrils. *PLoS One*. 2010;5(10):1-7. doi:10.1371/journal.pone.0015385

[32] Singh PK, Mora AK, Nath S. Ultrafast fluorescence spectroscopy reveals a dominant weakly-emissive population of fibril bound thioflavin-T. *Chem Commun*. 2015;51(74):14042-14045. doi:10.1039/c5cc04256a

[33] Adamcik J, Mezzenga R. Proteins Fibrils from a Polymer Physics Perspective - Macromolecules (ACS Publications). Published online 2012. http://pubs.acs.org/doi/abs/10.1021/ma202157h%5Cnpapers://e02909be-45fb-4c12-8160-f7962046a133/Paper/p3048

[34] Adamcik J, Mezzenga R. Study of amyloid fibrils via atomic force microscopy. *Curr Opin Colloid Interface Sci*. 2012;17(6):369-376. doi:10.1016/j.cocis.2012.08.001

[35] Kelly SM, Jess TJ, Price NC. How to study proteins by circular dichroism. *Biochim Biophys Acta - Proteins Proteomics*. 2005;1751(2):119-139. doi:10.1016/j.bbapap.2005.06.005

[36] Haris PI, Severcan F. FTIR spectroscopic characterization of protein structure in aqueous and non-aqueous media. *J Mol Catal - B Enzym*. 1999;7(1-4):207-221. doi:10.1016/S1381-1177(99)00030-2

[37] Melo AM, Coraor J, Alpha-Cobb G, et al. A functional role for intrinsic disorder in the tau-tubulin complex. *Proc Natl Acad Sci U S A*. 2016;113(50):14336-14341. doi:10.1073/pnas.1610137113

[38] Kapust RB, Tözsér J, Fox JD, et al. Tobacco etch virus protease: Mechanism of autolysis and rational design of stable mutants with wild-type catalytic proficiency. *Protein Eng*. 2001;14(12):993-1000. doi:10.1093/protein/14.12.993

[39] Manual I. QuikChange ® II XL Site-Directed Mutagenesis Kit. *Mutagenesis*. 2002;200521(5):1158-1160, 1162, 1164-1165. http://www.genomics.agilent.com/files/Manual/200521.pdf

[40] Nzytech. Protocol Nzytech. :4-7. https://www.nzytech.com/en/mb010-nzyminiprep/

[41] Pierce. BCA Protein Assay Kit 23225. 2020;(2161296):0-3. https://www.thermofisher.com/order/catalog/product/23225

[42] Furukawa Y, Kaneko K, Nukina N. Tau protein assembles into isoform- and disulfide-dependent polymorphic fibrils with distinct structural properties. *J Biol Chem*. 2011;286(31):27236-27246. doi:10.1074/jbc.M111.248963

[43] McClare CWF. An accurate and convenient organic phosphorus assay. *Anal Biochem*. 1971;39(2):527-530. doi:10.1016/0003-2697(71)90443-X

[44] Cleveland, D. W., Hwo, S. Y., and Kirschner, M. W. (1977). Physical and chemical properties of purified tau factor and the role of tau in microtubule assembly. *J. Mol. Biol.* 116, 227–247. doi: 10.1016/0022-2836(77)90214-5

[45] Danis C, Despres C, Bessa LM, et al. Nuclear magnetic resonance spectroscopy for the identification of multiple phosphorylations of intrinsically disordered proteins. *J Vis Exp*. 2016;2016(118):1-12. doi:10.3791/55001

[46] Elbaum-Garfinkle S, Cobb G, Compton JT, Li XH, Rhoades E. Tau mutants bind tubulin heterodimers with enhanced affinity. *Proc Natl Acad Sci U S A*. 2014;111(17):6311-6316. doi:10.1073/pnas.1315983111

[47] Zhu HL, Fernández C, Fan JB, et al. Quantitative characterization of heparin binding to tau protein: Implication for inducer-mediated tau filament formation. *J Biol Chem*. 2010;285(6):3592-3599. doi:10.1074/jbc.M109.035691

[48] Elbaum-Garfinkle S, Ramlall T, Rhoades E. The role of the lipid bilayer in tau aggregation. *Biophys J*. 2010;98(11):2722-2730. doi:10.1016/j.bpj.2010.03.013

[49] Chakraborty P, Rivière G, Liu S, et al. Co-factor-free aggregation of tau into seeding-competent RNA-sequestering amyloid fibrils. *Nat Commun*. 2021;12(1):1-12. doi:10.1038/s41467-021-24362-8

[50] Chen D, Drombosky KW, Hou Z, et al. Tau local structure shields an amyloid-forming motif and controls aggregation propensity. *Nat Commun*. 2019;10(1). doi:10.1038/s41467-019-10355-1

[51] Sallaberry CA, Voss BJ, Majewski J, et al. Tau and Membranes: Interactions That Promote Folding and Condensation. *Front Cell Dev Biol*. 2021;9(September):1-17. doi:10.3389/fcell.2021.725241

[52] Altendorf T, Gering I, Santiago-Schübel B, et al. Stabilization of Monomeric Tau Protein by All D-Enantiomeric Peptide Ligands as Therapeutic Strategy for Alzheimer's Disease and Other Tauopathies. *Int J Mol Sci*. 2023;24(3). doi:10.3390/ijms24032161